Response to comments:

We sincerely thank the reviewers for their helpful comments and guidance. Addressing the major points raised during the review process has substantially improved the quality of the manuscript. In the text that follows, reviewer comments in normal text are followed by author responses in italics.

Reviewer #1:

This manuscript presents measurements of aerosol composition made with an Aerodyne HRAMS in Houston, TX. The measurements were carried out in two different seasons, and the focus of the analysis is on differences in the OA composition and sources during these different times. Overall, this is a novel data set and the topic is certainly appropriate for ACP. The writing is generally good and the manuscript is well-organized. I do have a number of major issues with the manuscript – some addressed here, some in the section below – that prevent me from endorsing it for publication at this time. It may be suitable for publication after a major revision.

My greatest concern deals with the analyses and discussion related to Figure 9 (lines 482 - 494) and Figure 11 (lines 550 - 560). This seems like the definition of "cherry picking" data to support one's view, when the entire data set does not. There is no rationale for excluding such large amounts of data until one achieves a good linear fit. It supports the authors' narratives, but I think the conclusions involving these Figures (which are central to the entire manuscript) need substantial revision since they are not consistent with the data.

Response:

We thank the reviewer for highlighting this point, but we respectfully disagree with the reviewer that the data analysis involves cherry picking. Please note the fact that it is possible to find a distinct regression relationship between two observed variables for part of a given data set, in contrast to the whole data set. We can find many examples in the literature: for example, the third figure in Li et al. (2016) and the eighth figure in Guo et al. (2016). In this

work, OOA presented a non-linear relationship with LWC for our whole dataset, which is in agreement with a previous study (Xu et al., 2017). The main focus of their work was to investigate the effects of aqueous-phase and photochemical processing on secondary organic aerosol formation and evolution. Their data suggested that the OOA exhibited a non-linear relationship with RH for their whole dataset in different seasons. However, based on least squares regression correlation analysis, Sullivan et al. (2016) reported a relationship of an increasing water-soluble organic carbon with LWC for RH increased from 40% to 70% during a specific short period. Thus, our aim is to examine if there is a linear relationship between OOA and LWC during specific loadings of LWC.

Classical regression methods, such as linear least squares regression, were developed to specify a global function to fit a model to an entire data set. However, as mentioned by the reviewer, no rationale for determining what fraction of the data is appropriate for a good linear fit was provided. In general, data are usually chosen arbitrarily. Here we provide the detailed strategy for choosing the appropriate fraction of data points utilized in subsequent local linear regression analyses.

The first step is to examine the linear or non-linear relationships between two variables by fitting the given data with a locally weighted scatter plot smoothing algorithm (LOWESS). Further details on the LOWESS technique is available in Cleveland (1981). We take the relationship between LO-OOA and LWC during the summer campaign as an example. The LOWESS function has a "span" argument (f) that represents the proportion of the total number of points that contribute to each local fitted value. The fitting curve is constructed by connecting the "fitted" value with lines for each data point, with colors from red to blue to show the effect of the smoothing parameter choice. The red curve (f=0.01, where f is equal to the proportion of points) is "looser" than the blue curve (f=1), as the blue curve is fitted to all data points. As shown in Figure S14(C) (named as in the current SI), the blue curve fitted for data points with LWC concentration great than 5 $\mu g\ m^{-3}$ is likely a straight line. To further verify this assumption, we resampled the original data by using a bootstrap method and recalculated the LOWESS curves. Figure S14(D) presents the 400 LOWESS curves for all resampled data. A strong linear relationship between LO-OOA and LWC can be found for

data with LWC great than 6 μg m^{-3}. Because the number of the corresponding data points decreased as the LWC increased, the fitted curve is sparsely distributed for high LWC data. Although these resampled data points are not as representative compared to the data at lower LWC, the linear relationship is apparent.

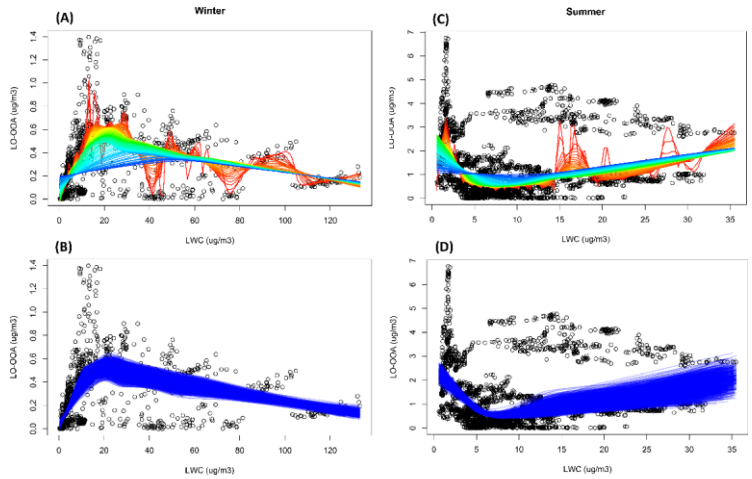

Figure S14. LOWESS curves for the nighttime LO-OOA vs. LWC during winter (A) and summer (C) and for the associated resampled data obtained by bootstrap method (B for winter and D for summer).

Author's changes in manuscript:

Our revision to this comment is included in the following bulleted list:

1. Added the results of LOWESS analysis into supplementary materials (Figures S14-17).

2. Added a paragraph before the discussion of Figure 8 to clarify the potential relationship between OOA and LWC during nighttime:

"The potential linear relationship between OOA and LWC for the nighttime data was investigated by fitting the data with a locally weighted scatter plot smoothing algorithm (LOWESS, (Cleveland, 1981)). According to the LOWESS curves fitted for the original nighttime data and the resampled data obtained by a bootstrap method (Figs. S14-15), there likely exists a linear relationship between LO-OOA and LWC for data points with LWC less

than 20 μg m^{-3} and greater than 6 μg m^{-3} for the winter and summer periods, respectively. As for MO-OOA, such a linear relationship likely exists when LWC is less than 50 and 7 μg m^{-3} for the winter and summer periods, respectively."

3. Added another paragraph before the discussion of Figure 10 to clarify the potential relationship between OOA and O_x during daytime:

"According to the LOWESS curves fitted for the original daytime data and resampled data obtained using a bootstrap method (Figs. S16-17), there likely exists a linear relationship between LO-OOA and O_x when O_x is less than 35 ppb and greater than 20 ppb for the winter and summer periods, respectively. As for MO-OOA, the linear relationship likely exists for data points with O_x less than 35 ppb for the winter period, but the linear relationship is less prominent."

4. Deleted the discussion of the linear relationship between MO-OOA and O_x for the summer campaign.

Specific comment 1:

I think that the quantification of the aerosol organic nitrates (ON) have a large uncertainty that needs to be discussed. Equations 3, 4, and 5 indicate the derived ON concentrations are very sensitive to the R_{ON} value. Although the authors have used an R_{ON} value from a very well cited source, there is major uncertainty because the source they cite is based upon a study of SOA from β-pinene oxidation by the nitrate radical. Clearly, the ON formation in this study will be more complex, which adds significant uncertainty to the R_{ON} value and thus to the derived ON concentrations. Much more discussion of this point, including bounds on the ON concentration is warranted.

Response:

Previous studies found that isoprene was the main biogenic VOC in Houston (Leuchner and Rappengluck, 2010; Kota et al., 2014), and Brown et al. (2013) reported that monoterpenes and isoprene were frequently present within the nocturnal boundary layer in the Houston area and underwent rapid oxidation, mainly by nitrate radical. Given the large abundance of

monoterpene and isoprene in the Houston area, similar to Xu et al. (2015), we assume organic nitrates formed via isoprene and beta-pinene oxidation are representative. Fry et al. (2013) assumed that the R_{ON}/R_{NH4NO3} value is instrument-independent, and further estimated the average R_{ON}/R_{NH4NO3} of 2.25 for the organic nitrate standards. The R_{ON}/R_{NH4NO3} values vary with precursor VOC. We utilized the average R_{ON}/R_{NH4NO3} of isoprene (2.08, (Bruns et al., 2010)) and beta-pinene organic nitrates (3.99, (Boyd et al., 2015)) from the literature to obtain an estimate range of R_{ON} by using the NO_x^+ method. The mass range of ON is estimated by assuming that the average molecular weights of organic molecules with nitrate functional groups are 200 to 300 g mol^{-1} (Surratt et al., 2008; Rollins et al., 2012).

The result of estimated ON is available in Table S2. The associated Figures and content in the original manuscript were updated accordingly. Here we retain the results estimated with R_{ON} value of 0.166 in the manuscript.

Table S2. Results of organic nitrates estimated using the NO_x^+ ratio method.

	$NO_{3,ON}$ conc. ($\mu g\ m^{-3}$)		$NO_{3,ON}/NO_{3,obs}$		ON/OA	
	lower	upper	lower	upper	lower	upper
Winter	0.22	0.34	34%	35%	31%	66%
Summer	0.05	0.06	61%	81%	9%	17%

Specific comment 2:

The COA factor seems quite problematic given that 1) it is present in winter but absent in summer (cooking is presumably still occurring in the city during this period?), and 2) the diurnal profile of COA (Fig. 4) is inconsistent with both cooking activity and results from many urban areas.

Response:

1) There is a restaurant situated directly northeast of the measurement site (UHSL). The northeasterly winds were observed at the measurement site with a high frequency during the winter campaign but not the summer (Fig. 1), which is likely to be responsible for the impact of emissions from cooking activities on this site during winter. It also is possible that increased

processing in the summer led COA to be oxidized and included in one of the OOA factors.

2) In our previous supplemental material, we have interpreted the COA factor by comparing the factor mass spectra with other factors, examining the relationship of COA factor versus cooking-tracer ion ($C_3H_3O^+$) and investigating the factor's signal ratio of m/z 55 to m/z 57. As shown in the following figure (now S13), the signals for m/z 55 to m/z 57 for COA in the summer is close to that for LO-OOA and MO-OOA, and higher than that for BBOA and HOA. This is a strong evidence for the interpretation of the COA factor (Mohr et al., 2012).

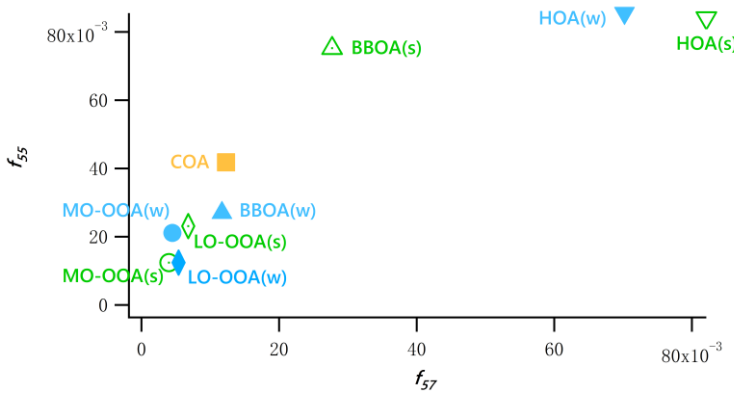

Figure S13. f_{55} vs. f_{57} of PMF factors for the winter and summer periods. (w) and (s) denote the winter and summer data, respectively.

Although there is no routine peak during mealtime in the diurnal pattern of COA, the COA factor mass spectra correlated moderately with previously reported COA factors deduced from PMF analysis (as shown in the table below), which further supports the interpretation of COA factor in this work.

Table Correlation (*r*) of COA mass spectra with previously published spectral database. (http://cires1.colorado.edu/jimenez-group/HRAMSsd/)

References	Study area	*r*
(Mohr et al., 2012)	Barcelona	0.76

(Crippa et al., 2013)	Paris	0.58
(Elser et al., 2016)	Xi'an and Beijing	0.65
(Hu et al., 2016)	Beijing	0.65

Specific comment 3:

The brief discussion on aerosol acidity (Lines 318-320) is completely wrong: briefly, the thermodynamic modeling did not include gas-phase ammonia or nitric acid, which significantly limits the ability to characterize acidity. See the extensive body of work form R. Weber and A. Nenes on this topic.

Response:

The original sentence (original lines 318-320) has been deleted.

Specific comment 4:

I had a lot of difficulty with Figure 1 and the associated discussion (Lines 349-360). I realize many published papers (including many in ACP) follow this standard formula for a paper reporting the results from a ground-based field study. However, I find it almost impossible to actually get anything useful out of Figure 1-there is simply too much data presented in too small a space. This is especially true for the discussions about pollutants and wind direction, which cannot be distinguished in Figure 1. If the discussion is central to the manuscript, then additional figures in the Supplemental and likely necessary. If not, then I'd suggest removing (or greatly modifying) Figure 1.

Response:

For the sake of clarity, we have removed the panels of elemental ratios (O/C, H/C, OM/OC, and N/C), ON and MSA from the stacked time series plot and put these panels into the supplemental material (Figure S2).

Specific comment 5:

Perhaps this is just a miscalculation, mis-labeled figure or a typo in the manuscript, but the ON concentration estimates (12% and 37% of OA) do not seem consistent with the results in Figure 2, Figure 6, and Table 1. For example, Fig. 2 lists ON contributions to NR-PM_1 as 3.4% and 1.5% in winter and summer, respectively. Based on the reported averages (NR-PM_1 concentrations of 6 and 3.6 $\mu g/m^3$ in winter and summer, respectively), this would give ON concentrations of 0.204 and 0.054 $\mu g/m^3$. These levels do not seen consistent with Figure 6, nor with the reported contributions to OA.

Response:

We apologize for the error. As suggested, we estimated the bounds of ON based on the R_{ON} values (and their precursor VOCs) that are relevant to the Houston area in the revised manuscript. The estimated result is available in Table S2. The ON concentrations in Tables, Figures and text have been updated in the revised manuscript.

Specific comment 6:

All of the discussion about wet removal is misguided (lines 448-452, 468). The authors seem to imply here that the highest levels of aerosol LWC correspond to periods of precipitation. I seriously doubt that is the case, as precipitation events will greatly reduce all of the aerosol species, as well. Either way, the authors should have access to accurate precipitation data, so this point should be backed by evidence rather than speculated upon.

Response:

Precipitation totals from a nearby Texas Commission on Environmental Quality (TCEQ) monitor site were added to Figure 1 (b, g). The periods of precipitation events correspond to high levels of RH. Indeed, the wet removal effect works on all species. We have rephrased the statement on wet removal effect in response to this comment.

Lines 436-441: "This result indicates that wet removal may dominate under an extremely high RH environment coupled with stagnant air (WS < 2 m/s, Fig. 7(E)), as the OA concentration

decreased at extremely high LWC level (Fig. 7(A)). In summer, the OA mass decreased when LWC increased from 1.25 to 6.25 μg m^{-3} but increased when LWC increased further, suggesting the wet removal effect is likely not as strong as that in winter because of the relatively lower LWC in summer."

Specific comment 7:

This discussion linking MSA with aqueous processing is confusing (lines 507-520). It is entirely possible for aqueous processing to produce OOA and at the same time for the OOA factors to exhibit weak (or no) correlations with MSA (e.g., if the air mass had a continental origin).

Response:

The discussion linking MSA with aqueous processing supports the idea that the summertime MO-OOA formation was more likely associated with aqueous processing than LO-OOA, as MO-OOA positively correlated with MSA but LO-OOA exhibited weak correlation with MSA. This result also indicates that MO-OOA was impacted by marine aerosol and that LO-OOA likely originated from continental areas.

Specific comment 8:

This is a relatively minor point, but I question the label of "summer" applied to the May measurements. Can the authors use comparison to priori measurement campaigns in Houston to show that May is representative of summertime conditions in terms of source influences, emissions, chemistry, etc.? Further, because of the short duration of the winter measurement period (2 weeks), the limitation that this campaign may not have fully characterized the winter season in Houston should be discussed.

Response:

We agree with the reviewer that the sampling periods are too short to cover the whole seasons thus we have added a comment in Section 2.1:

"The data collected during winter campaign are limited in duration; thus, the following discussion focuses primarily on the summer campaign. The label of "winter/summer" in the text denotes the measurement period in the winter/summer."

The fourth paragraph of the Introduction section has been deleted, and we have shortened the discussion about winter data in the text. It should also be noted that even though May officially is part of spring, the temperatures in Texas in May are high enough that they are much more characteristic of summer meteorology.

Specific comment 9:

The paragraph in lines 64-70 seems contradictory with the current results: the reported measurement seem to indicate that Houston is well below the current (and future) standard.

Response:

The original statement has been deleted.

Specific comment 10:

I understand that it is common to sample an AMS downstream of a Nafion drier (lines 150-152), but can the authors comment on potential artifacts from this measurement setup? E.g., the potential loss of semi-volatile organics.

Response:

The work of El-Sayed et al. (2016) indicates that drying of aerosol water led to the evaporation of condensed-phase organics (for both daytime and nighttime sampling periods). For the purposes of this study, therefore, we may be underestimating the contribution of aqueous-SOA (i.e., IEPOX as an example in El-Sayed et al. (2016)).

We have added comment in Section 2.3.2:

"As suggested by El-Sayed et al. (2016), drying of aerosol water may have led to the evaporation of condensed-phase organics. Thus, the mass concentrations of resolved OA factors here are a lower-bound, conservative estimate due to potential losses of aqueous-SOA

in the Nafion dryer element."

References:

Boyd, C. M., Sanchez, J., Xu, L., Eugene, A. J., Nah, T., Tuet, W. Y., Guzman, M. I., and Ng, N. L.: Secondary Organic Aerosol (SOA) formation from the β-pinene+NO_3 system: effect of humidity and peroxy radical fate, Atmos. Chem. Phys., 15, 7497–7522, doi:10.5194/acp-15-7497-2015, 2015.

Brown, S. S., Dube, W. P., Bahreini, R., Middlebrook, A. M., Brock, C. A., Warneke, C., de Gouw, J. A., Washenfelder, R. A., Atlas, E., Peischl, J., Ryerson, T. B., Holloway, J. S., Schwarz, J. P., Spackman, R., Trainer, M., Parrish, D. D., Fehshenfeld, F. C., and Ravishankara, A. R.: Biogenic VOC oxidation and organic aerosol formation in an urban nocturnal boundary layer: aircraft vertical profiles in Houston, TX, Atmos Chem Phys, 13, 11317-11337, 10.5194/acp-13-11317-2013, 2013.

Bruns, E. A., Perraud, V., Zelenyuk, A., Ezell, M. J., Johnson, S. N., Yu, Y., Imre, D., Finlayson-Pitts, B. J., and Alexander, M. L.: Comparison of FTIR and Particle Mass Spectrometry for the Measurement of Particulate Organic Nitrates, Environ. Sci. Technol., 44, 1056–1061, 2010.

Cleveland, W. S. (1981) LOWESS: A program for smoothing scatterplots by robust locally weighted regression. The American Statistician, 35, 54.

Crippa, M., El Haddad, I., Slowik, J. G., DeCarlo, P. F., Mohr, C., Heringa, M. F., Chirico, R., Marchand, N., Sciare, J., Baltensperger, U., and Prevot, A. S. H.: Identification of marine and continental aerosol sources in Paris using high resolution aerosol mass spectrometry, J Geophys Res-Atmos, 118, 1950-1963, 10.1002/jgrd.50151, 2013.

Elser, M., Huang, R. J., Wolf, R., Slowik, J. G., Wang, Q. Y., Canonaco, F., Li, G. H., Bozzetti, C., Daellenbach, K. R., Huang, Y., Zhang, R. J., Li, Z. Q., Cao, J. J., Baltensperger, U., El-Haddad, I., and Prevot, A. S. H.: New insights into $PM_{2.5}$ chemical composition and sources in two major cities in China during extreme haze events using aerosol mass spectrometry, Atmos Chem Phys, 16, 3207-3225, 10.5194/acp-16-3207-2016, 2016.

El-Sayed, M. M. H., Amenumey, D., and Hennigan, C. J.: Drying-Induced Evaporation of Secondary Organic Aerosol during Summer, Environ Sci Technol, 50, 3626-3633, 10.1021/acs.est.5b06002, 2016.

Fry, J. L., Draper, D. C., Zarzana, K. J., Campuzano-Jost, P., Day, D. A., Jimenez, J. L., Brown, S. S., Cohen, R. C., Kaser, L., Hansel, A., Cappellin, L., Karl, T., Roux, A. H., Turnipseed, A., Cantrell, C., Lefer, B. L., and Grossberg, N.: Observations of gas- and aerosol-phase organic nitrates at BEACHON-RoMBAS 2011, Atmos. Chem. Phys., 13, 8585-8605, http://doi.org/10.5194/acp-13-8585-2013, 2013.

Guo, H., Sullivan, A. P., Campuzano-Jost, P., Schroder, J. C., Lopez-Hilfiker, F. D., Dibb, J. E., Jimenez, J. L., Thornton, J. A., Brown, S. S., Nenes, A., and Weber, R. J.: Fine particle pH and the partitioning of nitric acid during winter in the northeastern United States, J Geophys Res-Atmos, 121, 10355-10376, 10.1002/2016jd025311, 2016.

Hu, W. W., Hu, M., Hu, W., Jimenez, J. L., Yuan, B., Chen, W. T., Wang, M., Wu, Y. S., Chen, C., Wang, Z. B., Peng, J. F., Zeng, L. M., and Shao, M.: Chemical composition, sources, and aging process of submicron aerosols in Beijing: Contrast between summer and winter,

J. Geophys. Res., 121, 1955-1977, http://doi.org/10.1002/2015jd024020, 2016.
Kota, S. H., Park, C., Hale, M. C., Werner, N. D., Schade, G. W., and Ying, Q.: Estimation of VOC emission factors from flux measurements using a receptor model and footprint analysis, Atmos Environ, 82, 24-35, 10.1016/j.atmosenv.2013.09.052, 2014.
Leuchner, M., and Rappengluck, B.: VOC source-receptor relationships in Houston during TexAQS-II, Atmos Environ, 44, 4056-4067, 10.1016/j.atmosenv.2009.02.029, 2010.
Li, X. G., Chen, W. F., Zhang, C. D., Li, Y., Wang, F. F., and Chen, W.: Enhanced dehydrochlorination of 1,1,2,2-tetrachloroethane by graphene-based nanomaterials, Environ Pollut, 214, 341-348, 10.1016/j.envpol.2016.04.035, 2016.
Mohr, C., DeCarlo, P. F., Heringa, M. F., Chirico, R., Slowik, J. G., Richter, R., Reche, C., Alastuey, A., Querol, X., Seco, R., Peñuelas, J., Jiménez, J. L., Crippa, M., Zimmermann, R., Baltensperger, U., and Prévôt, A. S. H.: Identification and quantification of organic aerosol from cooking and other sources in Barcelona using aerosol mass spectrometer data, Atmos. Chem. Phys., 12, 1649-1665, https://doi.org/10.5194/acp-12-1649-2012, 2012.
Rollins, A. W., Browne, E. C., Min, K. E., Pusede, S. E., Wooldridge, P. J., Gentner, D. R., Goldstein, A. H., Liu, S., Day, D. A., Russell, L. M., and Cohen, R. C.: Evidence for NO_x Control over Nighttime SOA Formation, Science, 337, 1210-1212, http://doi.org/10.1126/science.1221520, 2012.
Sullivan, A. P., Hodas, N., Turpin, B. J., Skog, K., Keutsch, F. N., Gilardoni, S., Paglione, M., Rinaldi, M., Decesari, S., Facchini, M. C., Poulain, L., Herrmann, H., Wiedensohler, A., Nemitz, E., Twigg, M. M., and Collett Jr, J. L.: Evidence for ambient dark aqueous SOA formation in the Po Valley, Italy, Atmos. Chem. Phys., 16, 8095-8108, http://doi.org/10.5194/acp-16-8095-2016, 2016.
Surratt, J. D., Gomez-Gonzalez, Y., Chan, A. W. H., Vermeylen, R., Shahgholi, M., Kleindienst, T. E., Edney, E. O., Offenberg, J. H., Lewandowski, M., Jaoui, M., Maenhaut, W., Claeys, M., Flagan, R. C., and Seinfeld, J. H.: Organosulfate formation in biogenic secondary organic aerosol, J. Phys. Chem. A, 112, 8345-8378, http://doi.org/10.1021/jp802310p, 2008.
Xu, L., Suresh, S., Guo, H., Weber, R. J., and Ng, N. L.: Aerosol characterization over the southeastern United States using high-resolution aerosol mass spectrometry: spatial and seasonal variation of aerosol composition and sources with a focus on organic nitrates, Atmos. Chem. Phys., 15, 7307-7336, http://doi.org/10.5194/acp-15-7307-2015, 2015.
Xu, W. Q., Han, T. T., Du, W., Wang, Q. Q., Chen, C., Zhao, J., Zhang, Y. J., Li, J., Fu, P. Q., Wang, Z. F., Worsnop, D. R., and Sun, Y. L.: Effects of Aqueous-Phase and Photochemical Processing on Secondary Organic Aerosol Formation and Evolution in Beijing, China, Environ. Sci. Technol., 51, 762-770, http://doi.org/10.1021/acs.est.6b04498, 2017.

Reviewer #2:

Specific Comment 1:

My major concern is that the authors claimed seasonal differences between winter and summer, but the measurements were only made for 2-week period during wintertime with high

frequencies of RH>60% (~70% in Fig.1). As a result, there might be a significant uncertainty when comparing the summer and winter data. The authors need to address such uncertainties in the revised manuscript.

Response:

Please see response to similar comment from Reviewer #1.

Specific Comment 2:

The uncertainties for the quantification of S/C and N/C AMS was operated in V-mode (m/Δm=~2000) in this study, separation of N-containing and S-containing are challenging. What are the uncertainties in quantification of S/C and N/C.

Response:

Because of the lack of measurement results for standard organic nitrates and organic sulfates, we are unable to estimate quantitatively the uncertainties in N/C and S/C. Since the elemental ratio packages in PIKA indicate that the calibration factors for S/C ratios are "not measured/published", we have deleted the S/C data in the revised manuscript.

The uncertainties in quantification of N/C include: 1) the important nitrogen-containing ion (CH_2N^+, m/z 28 (Ge et al., 2017)) was excluded from the AMS elemental analysis due to the overwhelming interference of adjacent N_2^+ ion, resulting in the current N/C ratio being underestimated by ~20% on average (Struckmeier et al., 2016); 2) because the signals of $C_xH_yN_p^+$ and $C_xH_yO_zN_p$+ are much lower than $C_xH_y^+$ and $C_xH_yO_z^+$, the determination of N/C relies on the mass resolution (m/Δm). The mass resolution of V-mode AMS is just half of that of W-mode, making separation and quantification of the nitrogen-containing ions above m/z 50 impossible (Xu et al., 2017); and 3) N-containing ion peaks are very often on tails of larger peaks, thus small errors in m/z calibration can generate uncertainty in estimated N/C.

Aiken et al. (2007) compared the N/C ratios for methylamine, ethylamine, and hydrogen cyanide from a NIST electron-ionization database and from elemental analysis using an AMS. The analysis of AMS (NIST) spectra indicates that quantification of N/C is possible with an

average error of 20%.

Specific Comment 3:

What the values of CE and RIE used for MSA quantification? Please elaborate.

Response:

Following previous studies by Zorn et al. (2008) and Huang et al. (2015), the relative ionization efficiency (RIE) of MSA (1.3) was assumed to be the average of the value for organic species (RIEorg = 1.4) and sulfate species (RIEso4 = 1.2). The collection efficiency of all ions composing MSA was calculated using the composition-dependent collection efficiency developed by Middlebrook et al. (2015). The resulting collection efficiency was 0.5 for 7.3% and 4.2% of time of the summer and winter campaign, respectively, and was 1.0 for the remaining time of the two campaigns.

Specific Comment 4:

What's the basis of LWC bin division (Fig.8)? Why didn't you use the uniformly-spaced LWC bin as Fig. 10 (Ox binned in 10 ppb).

Response:

Unlike the O_x concentration, the LWC in the winter and summer show a power function distribution and a lognormal distribution, respectively. We used uniformly-spaced LWC bins for most of the data. The summer data are binned in 5 $\mu g\ m^{-3}$ increments from 0 to 20 $\mu g\ m^{-3}$ (covering 83% of data points), and winter data are binned in 2.5 $\mu g\ m^{-3}$ increments from 0 to 15 $\mu g\ m^{-3}$ (covering 91% of data points). The number of data points within each bin is too small to produce a reasonable result if the remaining data at higher values are binned using the same increment. This data processing method is common in literature (Huang et al., 2015).

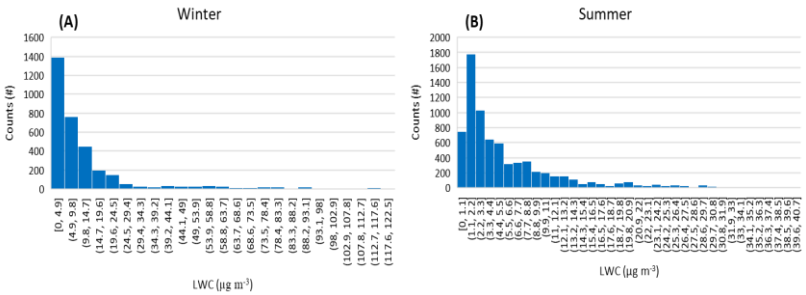

406

407 **Figure** The frequency histograms of LWC in the winter and summer.

408

409 **Specific Comment 5:**

410 Are there any specific reasons that you used two different versions of software to do data
411 analysis (PIKA1.16 for time series (line 176) and PIKA 1.19D to do PMF analysis (line 235))?

412

413 *Response:*

414 *We performed updated data analysis in the version of PIKA 1.19D, and all data presented in*
415 *Figures, Tables and the text have been updated in the revised manuscript.*

416

417 **Specific Comment 6:**

418 How the density of organics was calculated? Was it the I-A method (you mentioned in line
419 183?) or A-A methods?

420

421 *Response:*

422 *The organic density was estimated using an empirical equation based on elemental ratios*
423 *(Kuwata et al., 2012):*

424 $$\rho_{Org} = 1000 \times [\frac{12+\frac{H}{C}+16\times\frac{O}{C}}{7.0+5\times\frac{H}{C}+4.15\times\frac{O}{C}}]$$

425 *The elemental ratios were estimated using the updated I-A method (Canagaratna et al., 2015).*

426

427 **Specific Comment 7:**

428 Line 199-200, NO_2^+/NO^+=0.1-2.0, that is to say, the NO^+/NO_2^+= 0.5-10, which is

contradictory with the cited study (5-10) (Xu et al., 2015). What is the ON with R_{ON}=0.5? Please mention it here.

Response:

This is an error. The NO_2^+/NO^+ ratio is in the range of 0.1-0.2. This mistyping has been deleted and the bounds of ON have been estimated. Please see response to Reviewer #1 regarding uncertainties in ON.

Specific Comment 8:

Line 417, what is the correlation coefficient between LO-OOA/MO-OOA vs. aq-OOA in summer? Are there any further support other than the mass spectra? In fact, the correlation between LO-OOA/MO-OOA vs. SO_4 is moderate in Fig. 7.

Response:

The correlation coefficients of summertime LO-OOA/MO-OOA mass spectra with aq-OOA is 0.95/0.96, respectively. This result suggests that the formation of LO-OOA in summer and MO-OOA in both seasons likely involved aqueous processing. The correlation between OOA and MSA also supports this. MSA has a relatively higher correlation coefficient with MO-OOA (r=0.45) compared to LO-OOA (r=0.30), though the correlation also is influenced by many other factors. Additionally, the high correlation coefficients of SO_4 with MO-OOA in both seasons (r=0.74 and 0.79 for winter and summer, respectively) further support the conclusion, although the correlation of LO-OOA and SO_4 is not as strong as expected. We believe that the strong correlation between the mass spectra of OOA and aq-OOA is strong enough to support our conclusion.

Specific Comment 9:

Line 448, the authors attributed the decreased MO-OOA concentration at LWC > 40 μg/m^3 to wet removal. How about other species? Besides, in Fig.8 (I), the continuous increase of MO-OOA under LWC < 40 μg/m^3 appeared not very clear.

Response:

Please see response to Reviewer #1. The continuous increase of MO-OOA under LWC< 40 μg m^{-3} is not very clear, but the maximum and minimum values of each bin increased obviously. We further investigated the relationship between MO-OOA and LWC for nighttime data only, and the MO-OOA shows a significant increase trend under LWC< 40 μg m^{-3} during nighttime.

References:

Aiken, A. C., DeCarlo, P. F., and Jimenez, J. L.: Elemental Analysis of Organic Species with Electron Ionization High Resolution Mass Spectrometry, Anal. Chem., 79, 8350–8358, doi:10.1021/ac071150w, 2007.

Canagaratna, M. R., Jimenez, J. L., Kroll, J. H., Chen, Q., Kessler, S. H., Massoli, P., Hildebrandt Ruiz, L., Fortner, E., Williams, L. R., Wilson, K. R., Surratt, J. D., Donahue, N. M., Jayne, J. T., and Worsnop, D. R.: Elemental ratio measurements of organic compounds using aerosol mass spectrometry: characterization, improved calibration, and implications, Atmos. Chem. Phys., 15, 253-272, http://doi.org/10.5194/acp-15-253-2015, 2015.

Ge, X. L., Li, L., Chen, Y. F., Chen, H., Wu, D., Wang, J. F., Xie, X. C., Ge, S., Ye, Z. L., Xu, J. Z., and Chen, M. D.: Aerosol characteristics and sources in Yangzhou, China resolved by offline aerosol mass spectrometry and other techniques, Environ Pollut, 225, 74-85, 10.1016/j.envpol.2017.03.044, 2017.

Huang, D. D., Li, Y. J., Lee, B. P., and Chan, C. K.: Analysis of Organic Sulfur Compounds in Atmospheric Aerosols at the HKUST Supersite in Hong Kong Using HR-ToF-AMS, Environ Sci Technol, 49, 3672-3679, 10.1021/es5056269, 2015.

Kuwata, M., Zorn, S. R., and Martin, S. T.: Using Elemental Ratios to Predict the Density of Organic Material Composed of Carbon, Hydrogen, and Oxygen, Environ. Sci. Technol., 46, 787-794, http://doi.org/10.1021/es202525q, 2012.

Middlebrook, A. M., Bahreini, R., Jimenez, J. L., and Canagaratna, M. R.: Evaluation of Composition-Dependent Collection Efficiencies for the Aerodyne Aerosol Mass Spectrometer using Field Data, Aerosol Sci Tech, 46, 258-271, 10.1080/02786826.2011.620041, 2012.

Struckmeier, C., Drewnick, F., Fachinger, F., Gobbi, G. P., and Borrmann, S.: Atmospheric aerosols in Rome, Italy: sources, dynamics and spatial variations during two seasons, Atmos Chem Phys, 16, 15277-15299, 10.5194/acp-16-15277-2016, 2016.

Xu, L., Suresh, S., Guo, H., Weber, R. J., and Ng, N. L.: Aerosol characterization over the southeastern United States using high-resolution aerosol mass spectrometry: spatial and seasonal variation of aerosol composition and sources with a focus on organic nitrates, Atmos. Chem. Phys., 15, 7307-7336, http://doi.org/10.5194/acp-15-7307-2015, 2015.

Xu, W. Q., Sun, Y. L., Wang, Q. Q., Du, W., Zhao, J., Ge, X. L., Han, T. T., Zhang, Y. J., Zhou,

W., Li, J., Fu, P. Q., Wang, Z. F., and Worsnop, D. R.: Seasonal Characterization of Organic Nitrogen in Atmospheric Aerosols Using High Resolution Aerosol Mass Spectrometry in Beijing, China, Acs Earth Space Chem, 1, 673-682, 10.1021/acsearthspacechem.7b00106, 2017.

Zorn, S. R., Drewnick, F., Schott, M., Hoffmann, T., and Borrmann, S.: Characterization of the South Atlantic marine boundary layer aerosol using an aerodyne aerosol mass spectrometer, Atmos. Chem. Phys., 8, 4711-4728, https://doi.org/10.5194/acp-8-4711-2008, 2008.

Seasonal differences in formation processes of oxidized organic aerosol near Houston, TX

Qili Dai[1, 2], Benjamin C. Schulze[2, 3], Xiaohui Bi[1, 2], Alexander A.T. Bui[2], Fangzhou Guo[2], Henry W. Wallace[2, 4], Nancy P. Sanchez[2], James H. Flynn[5], Barry L. Lefer[5, 6], Yinchang Feng[1*], Robert J. Griffin[2, 7]

[1] State Environmental Protection Key Laboratory of Urban Ambient Air Particulate Matter Pollution Prevention and Control, College of Environmental Science and Engineering, Nankai University, Tianjin 300350, China

[2] Department of Civil and Environmental Engineering, Rice University, Houston, TX, 77005

[3] Now at Department of Environmental Science and Engineering, California Institute of Technology, Pasadena, CA, 91125

[4] Now at Washington State Department of Ecology, Lacey WA, 98503

[5] Department of Earth and Atmospheric Sciences, University of Houston, Houston, TX, 77004

[6] Now at Division of Tropospheric Composition, NASA, Washington, DC 20024

[7] Department of Chemical and Biomolecular Engineering, Rice University, Houston, TX, 77005

[*]Corresponding author: Yinchang Feng (fengyc@nankai.edu.cn)

Abstract

Submicron aerosol was measured to the southwest of Houston, Texas during winter and summer 2014 to investigate its seasonal variability. Data from a high-resolution time-of-flight aerosol mass spectrometer (HR-ToF-AMS) indicated that organic aerosol (OA) was the largest component of non-refractory submicron particulate matter (NR-PM_1) (on average, ~~46~~ 38 ± 13% and ~~55~~ 47 ± 18% of the NR-PM_1 mass loading in winter and summer, respectively). Positive matrix factorization (PMF) analysis of the OA mass spectra demonstrated that two classes of oxygenated OA (less and more-oxidized OOA, LO and MO) together dominated OA mass in summer (77%) and accounted for ~~42~~39% of OA mass in winter. The fraction of LO-OOA (out of total OOA) is higher in summer (~~69~~70%) than in winter (44%). Secondary aerosols (sulfate+nitrate+ammonium+OOA) accounted for ~76% and ~~89~~88% of NR-PM_1 mass in winter and summer, respectively, indicating NR-PM_1 mass was driven mostly by secondary aerosol formation regardless of the season. The mass loadings and diurnal patterns of these secondary aerosols show a clear winter/summer contrast. Organic nitrate (ON) concentrations were estimated using the NO_x^+ ratio method, with ~~an average~~ contributions of 31-66~~~15~~% and 9-17~~37~~% to OA during winter and summer campaign, respectively. The estimated ON in summer strongly correlated with LO-OOA (r= 0.73) and was enhanced at nighttime.

The relative importance of aqueous-phase chemistry and photochemistry in processing OOA was investigated by examining the relationship of aerosol liquid water content (LWC) and the sum of ozone (O_3) and nitrogen dioxide (NO_2) (O_x=O_3+NO_2) with LO-OOA and MO-OOA. The processing mechanism of LO-OOA apparently depended on relative humidity (RH). In periods of RH <80%, aqueous-phase chemistry likely played an important role in the

formation of wintertime LO-OOA, whereas photochemistry promoted the formation of summertime LO-OOA. For periods of high RH >80%, these effects were opposite that of low RH periods. Both photochemistry and aqueous-phase processing appear to facilitate MO-OOA formation except during periods of high LWC, which is likely a result of wet removal during periods of light rain.

The nighttime increases of MO-OOA during winter and summer were 0.013 and 0.01 μg MO-OOA per μg of LWC, respectively. The increase of LO-OOA was larger than that for MO-OOA, with increase rates of 0.033 and 0.055 μg LO-OOA per μg of LWC at night during winter and summer, respectively. On average, the mass concentration of LO-OOA in summer was elevated by nearly 1.2 μg m^{-3} for a ~20 μg change in LWC, which is accompanied by a 40 ppb change in O_x.

1 Introduction

Tropospheric particulate matter (PM) has adverse effects on air quality, visibility, and ecosystems and participates in climate forcing (Watson, 2002; Grantz et al., 2003; Racherla and Adams, 2006; Tai et al., 2010; Liu et al., 2017). The various effects of PM depend on its physical, chemical and optical properties, which are determined by its emission, formation and evolution/aging processes. Atmospheric PM can either be directly emitted from primary sources (fossil fuel combustion, soil dust, sea salt, biomass burning, etc.) or formed through chemical reactions of gaseous precursors, as is the case for secondary inorganic sulfate (SO_4^{2-}) and nitrate (NO_3^-) and secondary organic aerosol (SOA). Understanding the source

contributions and formation pathways of PM is essential for mitigating its effects (Jimenez et al., 2009).

Houston, TX, is of great interest to the scientific community with respect to air quality, as it is the fourth most populous city in the United States (U.S.) and is well known for its energy and chemical industries. ~~The annual average National Ambient Air Quality Standard (NAAQS) for $PM_{2.5}$ (PM with diameter smaller than 2.5 micron) set by the U.S. Environmental Protection Agency (EPA) was recently tightened from 15 to 12 μg m^{-3} (US EPA, 2013), causing Houston to be near non-attainment of this new standard, and creating a challenging for future NAAQS attainment (Bean et al., 2016).~~

Numerous efforts, from modelling (McKeen et al., 2009; Li et al., 2015; Ying et al., 2015) to field measurements (for example, TexAQS 2000 and II (Bates et al., 2008; Parrish et al., 2009; Atkinson et al., 2010), Go-MACCS (McKeen et al., 2009; Parrish et al., 2009), TRAMP2006 (Mao et al., 2010; Cleveland et al., 2012), GC-ARCH (Allen and Fraser, 2006), SHARP (Olaguer et al., 2014), and DISCOVER-AQ (Bean et al., 2016; Leong et al., 2017)) have been made in the Houston metropolitan area during the past two decades, providing critical insights into our understanding of air quality and atmospheric chemistry with respect to the sources and formation of PM. Previous field campaigns underscore that OA accounts for a major fraction of non-refractory submicron PM (NR-PM_1) in Houston (Bates et al., 2008; Russell et al., 2009; Cleveland et al., 2012; Brown et al., 2013; Bean et al., 2016; Leong et al., 2017; Wallace et al., 2018). The spatial variation of NR-PM_1 in Houston was investigated by Leong et al. (2017), who divided ~~the~~ greater Houston into two zones based on marked differences in NR-PM_1 levels, characteristics, and dynamics measured at 16 sampling locations.

589 Zone 1 is northwest of Houston and is dominated by SOA likely driven by nighttime biogenic
590 organic nitrate (ON) formation. Intensive attention has been paid recently to such
591 anthropogenic-biogenic interactions (Bahreini et al., 2009; Bean et al., 2016). Zone 2 is the
592 industrial/urban area south/east of Houston. Wallace et al. (2018) found mobile source exhaust
593 and petrochemical emissions likely are the most important factors impacting the NR-PM_1 and
594 trace gases at a site in Zone 2.

595 ~~In terms of seasonal variation, many aerosol mass spectrometer (AMS) field campaigns~~
596 ~~worldwide have been conducted in the summer (de Gouw et al., 2008; Takegawa et al., 2009;~~
597 ~~Lefer et al., 2010; Crippa et al., 2013a; Hayes et al., 2013; Hu et al., 2016). Intense summertime~~
598 ~~photochemical activity in Houston was observed during TRAMP 2006 relative to other field~~
599 ~~studies (Mao et al., 2010), indicating the potential important role of photochemical oxidation in~~
600 ~~SOA formation in the summer (Bahreini et al., 2009). In contrast, few measurements have~~
601 ~~focused on wintertime aerosol (Crippa et al., 2013b; Chakraborty et al., 2015; Kim et al., 2017;~~
602 ~~Wallace et al., 2008). Wintertime aerosol generally exhibits elevated mass loadings due to the~~
603 ~~enhanced emissions from fuel combustion for heating and weather conditions favorable to~~
604 ~~aerosol accumulation. Only a few studies present results based on long-term measurements for~~
605 ~~seasonal comparison, such as in the SE U.S. (Xu et al., 2015; Budisulistiorini et al., 2016). The~~
606 ~~knowledge gap regarding aerosol seasonal variability in Houston needs to be addressed to~~
607 ~~improve regional air quality.~~

608 Formation of SOA in clouds and the aqueous phase of aerosol particles has been reported
609 worldwide (Lim et al., 2010; Ervens et al., 2011; Xu et al., 2017). Given that both
610 photochemical oxidation and aqueous-phase chemistry are conducive to the formation of SOA,

it is of interest to compare the relative importance of photochemistry and aqueous-phase chemistry for SOA formation in different seasons. The roles of photochemistry and aqueous-phase processing on SOA formation and evolution in different seasons in Beijing have been investigated by Hu et al. (2016) and Xu et al. (2017), respectively. Generally, the aqueous-phase processing has a dominant influence on the formation of more oxidized SOA and photochemical chemistry plays a major role in the formation of less oxidized SOA in summer and winter in Beijing, while the relative importance of these two pathways in the formation processes of SOA in autumn is different from those in summer and winter. The relative roles of aqueous-phase and photochemical processes in the formation of SOA likely vary with location and time. The seasonal differences in the spectral patterns, oxidation degrees and contributions of SOA may result from different VOCs precursors, meteorological conditions and atmospheric oxidizing capacity, which are not well understood in Houston, particularly in different seasons.

This study presents observations of NR-PM_1 from two high-resolution time-of-flight AMS (HR-ToF-AMS) measurement campaigns conducted during the winter and summer of 2014 at a site in the suburbs of Houston, where industrial and vehicular emission sources and photochemical processes are likely to play an important role in NR-PM_1 formation (Leong et al., 2017). In addition to local emissions, this site was possibly impacted by regional marine aerosol transported from the Gulf of Mexico (Schulze et al., 2018). The aims of this work are to (1) investigate the seasonal characteristics of NR-PM_1 in the Houston area, (2) characterize the primary and secondary sources by applying positive matrix factorization (PMF) analysis to the measured OA mass spectra, and (3) evaluate the seasonal dependence of SOA composition and

633 formation, with a main focus on the relative effects of photochemistry and aqueous-phase
634 chemistry.
635
636 ## 2 Materials and Methods
637 ### 2.1 Sampling Site and Campaigns
638 Instrumentation was deployed in the University of Houston/Rice University Mobile Air
639 Quality Laboratory (MAQL), as described in Leong et al. (2017) and Wallace et al. (2018). The
640 winter campaign was conducted from February 3 through February 17, 2014, and the summer
641 campaign was conducted from May 1 to May 31, 2014. The measurement site was located on
642 the campus of University of Houston Sugar Land (UHSL) (29.5740 °N, 95.6518 °W). The
643 campus is situated southwest of downtown and the Houston Ship Channel (HSC). The map of
644 the measurement site is presented in Fig. S1 in the Supplemental Information (SI). The nearby
645 interstate highway (I-69) extends to the west of downtown and serves as a major traffic
646 emission source. The W.A. Parish Generating Station, a coal-fired power plant that is the
647 largest electricity generating facility in Texas, is ~6 miles south of the site (Fig. S1). The data
648 collected in the winter campaign is limited, thus the following discussion is focus primarily on
649 the summer campaign. The label of "winter/summer" in the text denotes the measurement
650 period in the winter/summer.
651 ### 2.2 Measurements
652 The data used in this paper are reported in local time, which is 6 and 5 hours behind
653 Universal Coordinated Time ~~(UTC)~~ in winter and summer, respectively. The details regarding

654 the instrumental setup and data processing of these measurements were the same as described
655 in Wallace et al. (2018). The NR-PM_1 composition was measured using an Aerodyne
656 HR-ToF-AMS (DeCarlo et al., 2006; Canagaratna et al., 2007). A $PM_{2.5}$ Teflon®-coated
657 cyclone inlet was installed above the MAQL trailer at a height of 6 m above ground to remove
658 coarse particles and to introduce air into the sampling line at a rate of 16.7 SLPM. A Nafion
659 dryer (Perma Pure, LLC) was mounted upstream of the HR-ToF-AMS to dry the sample to
660 below 45% relative humidity (RH). Particles are focused into a narrow beam via an
661 aerodynamic lens and accelerated under high vacuum into the particle sizing measurement
662 chamber. After passing the particle sizing chamber, the non-refractory components are flash
663 vaporized at near 600^{o}C and ionized using electron impact at 70 eV. Ionized mass fragments are
664 then transmitted directly into the time-of-flight region so that the mass spectra can be obtained.
665 In this study, the HR-ToF-AMS was operated in "V-mode" to obtain the non-refractory
666 chemical components with a higher sensitivity, lower mass spectral resolution compared to the
667 "W-mode." Ionization efficiency (IE) calibration was performed monodisperse ammonium
668 nitrate (NH_4NO_3) at the beginning and end of each campaign. Filtered ambient air was sampled
669 every two days for approximately 20 to 30 min to provide a baseline of signal for the
670 HR-ToF-AMS during campaigns. The detection limits, (Table S1 in the SI) were calculated by
671 multiplying the standard deviations of the filter periods by three.

672 Trace gas mixing ratios and meteorological parameters also were measured on the MAQL
673 during the campaigns. Carbon monoxide (CO) was measured with high-resolution cavity
674 enhanced direct-absorption spectroscopy (Los Gatos Research, Inc.), and sulfur dioxide (SO_2)
675 was quantified using a pulsed fluorescence analyzer (ThermoFischer Scientific, model

43i-TLE). Nitric oxide (NO) and nitrogen dioxide (NO_2) were measured with a chemiluminescence monitor with a UV-LED NO_2 photolytic converter on the NO_2 channel (AQD, Inc.) The total reactive nitrogen (NO_y) was measured with a Thermo 49c-TL with a heated Mo inlet converter. Ozone (O_3) mixing ratio was measured with ultraviolet absorption (2BTech, Inc., model 205). Meteorological parameters including ambient temperature, solar radiation, RH, wind speed (WS), and wind direction were measured using an RM Young meteorological station. Precipitation totals from a nearly Texas Commission on Environmental Quality (TCEQ) monitor site (EPA Site: 48_157_0696) were downloaded from TECQ website.

2.3 Data Processing

The HR-ToF-AMS data analysis was performed using SQUIRREL v.1.56A and PIKA v.1.~~16~~ 19D in Igor Pro 6.37 (Wave Metrics Inc.). The relative ionization efficiencies (RIE) were applied to OA (1.4), SO_4^{2-} (1.2), NO_3^- (1.1), NH_4^+ (4.0), and chloride (Cl^-, 1.3) following the standard data analysis procedures. The composition-dependent collection efficiency (CE) was applied to the data based on Middlebrook et al. (2012). Elemental ratios (H/C, O/C~~,~~ and N/C~~, and S/C~~, where H is hydrogen, C is carbon, N is nitrogen~~, and S is sulfur~~) and the ratio of organic mass to organic carbon (OM/OC) were generated using the procedures described by Canagaratna et al. (2015).

2.3.1 Quantification of the contributions of ON and Methanesulfonic Acid (MSA)

Estimation of ON. The mass loading of NO_3^- measured by HR-ToF-AMS includes both organic and inorganic NO_3^-. The fragmentation ratio of NO_2^+ to NO^+ (NO_x^+ ratio) is different for ON and inorganic NO_3^- (Farmer et al., 2010; Fry et al., 2013), and the NO_2^+ and NO^+ mass

loadings for ON ($NO_{2,ON}$ and NO_{ON}) can be estimated using the method proposed by Farmer et al. (2010):

$$NO_{2,ON} = \frac{NO_{2,obs} \times (R_{obs} - R_{NO_3NH_4})}{R_{ON} - R_{NO_3NH_4}} \quad (1)$$

$$NO_{ON} = NO_{2,ON} / R_{ON} \quad (2)$$

where R_{obs} is the ambient NO_x^+ ratio (0.531, 0.260 for the winter and summer campaign, respectively, see Fig. S2 for details). $R_{NO_3NH_4}$(NO_x^+ ratio of NH_4NO_3) is determined by IE calibration using monodisperse NH_4NO_3 before and after the campaigns. The average of the two IE calibrations was used as the $R_{NO_3NH_4}$ for the campaign (0.588, 0.381 for the winter and summer campaigns, respectively), which is comparable with the value reported elsewhere (Xu et al., 2015; Zhu et al., 2016). The value of R_{ON} is hard to determine because it varies with instruments and precursor volatile organic compounds (VOCs) (Fry et al., 2013). Previous studies have found that isoprene was the main biogenic VOC in Houston (Leuchner and Rappengluck, 2010; Kota et al., 2014), and Brown et al. (2013) reported that monoterpenes and isoprene were frequently present within the nocturnal boundary layer in Houston area and underwent rapid oxidation, mainly by nitrate radical (denoted as $NO_3^{\cdot}$ with a dot to differentiate it from aerosol NO_3^-). Given the abundance of monoterpene and isoprene in Houston area, similar to Xu et al. (2015), we assume organic nitrates formed via isoprene and beta-pinene oxidation are representative. Fry et al. (2013) assumed that the $R_{ON}/R_{NH_4NO_3}$ value is instrument-independent, and further estimated the average $R_{ON}/R_{NH_4NO_3}$ of 2.25 for the organic nitrate standards. The $R_{ON}/R_{NH_4NO_3}$ values vary with precursor VOC. We utilized the average $R_{ON}/R_{NH_4NO_3}$ of isoprene (2.08, (Bruns et al., 2010)) and beta-pinene organic nitrates (3.99,

带格式的: 下标

带格式的: 下标

带格式的: 上标

(Boyd et al., 2015)) from the literatures to obtain an estimation range of R_{ON} by using the NO_x^+ method.

~~As summarized by Xu et al. (2015), R_{ON} values ranging from 0.1 to 2.0 likely correspond to the upper and lower bounds of the ON concentration estimated by the NO_x^+ ratio method. In this work, R_{ON} is adopted as 0.166 as reported in literature (Fry et al., 2009). In winter, R_{OBS} was significantly higher than R_{ON} and close to $R_{NO_3NH_4}$, implying significant existence of inorganic NO_3^-. In summer, R_{OBS} was lower than $R_{NO_3NH_4}$ and close to R_{ON}, indicating a significant fraction of the total NO_3^- is ON (Fig. S2).~~

The measured NO_x^+ ratio can be used to separately quantify ammonium and organic nitrates as:

$$ON_{frac} = \frac{(R_{obs} - R_{NO3NH4})(1+R_{ON})}{(R_{ON} - R_{NO3NH4})(1+R_{obs})} \quad (3)$$

The nitrate functionality from organic nitrate was calculated as:

$$NO_{3,ON} = ON_{frac} \times NO_3^- \quad (4)$$

Thus, the nitrate functionality from inorganic nitrate (assuming NH_4NO_3 is the solely important inorganic nitrate in the submicron mode) can be calculated as:

$$NO_{3,AN} = \left(1 - ON_{frac}\right) \times NO_3^- \quad (5)$$

The accurate estimation of the total mass of ON via this method is uncertain as the actual molecular weight of the particle-phase species is unclear. Generally, the mass of ON is estimated by assuming that the average molecular weights of organic molecules with nitrate functional groups (value determined as described above) are 200 to 300 g mol^{-1} (Surratt et al., 2008; Rollins et al., 2012). Previous work found that the nitrate radical (denoted as $NO_3^{\cdot}$ with a dot to differentiate it from aerosol NO_3^-) reaction with monoterpenes resulted in significant

SOA formation and that a hydroperoxy nitrate ($C_{10}H_{17}NO_5$) was likely a major $NO_3^{\cdot}$-oxidized terpene product in the southeastern U.S. (Ayres et al., 2015). Here, we use the molecular weight of $C_{10}H_{17}NO_5$ (231 g mol^{-1}) to calculate the ON mass. Example periods of significant ON contribution to PM are given in Fig. S3. While the values of ON concentrations estimated using the method are presented in the text, the result of estimated ON including uncertainties is available in Table S2.

Estimation of MSA. During the two campaigns, there is no significant organic sulfur contribution from other ion fragments except for $CH_3SO_2^+$. The concentration of MSA was estimated as:

$$C_{MSA} = \frac{C_{CH3SO2}}{f_{MSA,CH3SO2}} \quad (6)$$

where C_{CH3SO2} is the concentration of ion fragment $CH_3SO_2^+$ (*m/z*=78.99) and the fraction of $CH_3SO_2^+$ to the total signal intensity of all the fragments of pure MSA, $f_{MSA,CH3SO2}$, is 5.55%. This values was observed for the mass spectra of pure MSA in laboratory experiments (Schulze et al., 2018) and is comparable to previous work (Huang et al., 2015).

2.3.2 Positive Matrix Factorization (PMF) Analysis

The PMF technique has been used widely for source apportionment (Paatero and Tapper, 1994), including with HR-TOF-AMS data (Ulbrich et al., 2009; Zhang et al., 2011). The high-resolution NR-PM_1 OA mass spectra matrix (m/z =12 to m/z=130) and the associated error matrix obtained by using PIKA v 1.19 D were used for PMF analysis. Data were prepared according to the protocol proposed by Ulbrich et al. (2009) and Zhang et al. (2011) prior to

PMF analysis. The PMF model was used to decompose the measured OA mass spectra matrix by solving:

$$X = GF + E = \sum_{p=1}^{J} G_{ip} F_{pj} + E_{ij} \quad (7)$$

where X is the $m \times n$ matrix of measurement data, the *m* rows of X are the OA mass spectra measured at each time step, the *n* columns of X are the time series of each organic mass-to-charge ratio, and p is the number of factors. G_{ip} is the matrix that denotes the contributions of factor p at time step i, and F_{pj} represents the factor mass spectral profiles. E is the residual matrix. The least-squares algorithm is used to fit the data to minimize iteratively a quality of fit parameter, Q:

$$Q = \sum_I \sum_J (E_{ij}/\sigma_{ij})^2 \quad (8)$$

where σ_{ij} is the matrix of estimated errors of the data.

Solutions using PMF with 2 to 7 factors were explored. The best solution with the optimum number of factors was evaluated carefully using an open source PMF evaluation tool (PET v 2.08D, (Ulbrich et al., 2009)) following the procedures described in Zhang et al. (2011). Selection criteria included 1.) variation of the ratio of Q to expected Q_{exp} ($mn-p(m+n)$, the degrees of freedom of the fitted data (Paatero et al., 2002)) after adding an additional factor, 2.) agreement between the reconstructed OA mass concentrations and the measured concentrations, 3.) scaled residuals for the different ion fragments included in the dataset and variations of the residual of the solution as a function of time, 4.) agreement between factor time series and time series of external tracers/individual ions, and 5.) examination of factor profiles. The last two are considered to determine the physical meaningfulness of the factors. The PMF solution with

781 factor numbers greater than five and four for winter and summer dataset, respectively, yielded
782 no new distinct and physical meaningful factors. The Q/Q_{exp} and the factors obtained for
783 different FPEAK (from -1 to 1 with a step value of 0.2) values resulted in a small difference in
784 the OA components. Because of the lowest Q/Q_{exp} and because the use of FPEAK values
785 different from 0 did not improve the correlations between PMF factors and potentially
786 associated tracers, the five- and four-factors solutions with FPEAK=0 can be well interpreted in
787 winter and summer, respectively. The convergence of the PMF model containing five- and
788 four-factors were examined by running each model from fifteen different starting values
789 (SEEDs 0-30 with a step value of 2). The small variation observed in Q/Q_{exp} and the mass
790 fraction of different factors as SEED changed indicates the solutions were stable. As a result,
791 SEED 0 was chosen for the final solution. The factors were interpreted as hydrocarbon-like OA
792 (HOA), biomass burning OA (BBOA), cooking OA (COA, identified only in the winter
793 campaign), and two oxidized OA (named less-oxygenated (LO-) OOA and more-oxygenated
794 (MO-) OOA). The data treatment, factor selection and interpretation are detailed in the SI. As
795 suggested by El-Sayed et al. (2016), drying of aerosol water may have led to the evaporation of
796 condensed-phase organics. Thus, the resolved mass concentrations of OA factors here are a
797 lower-bound, conservative estimate due to losses of aqueous-SOA in the dryer element.

798 **2.3.3 Estimation of Aerosol Liquid Water Content (LWC)**

799 Aerosol LWC includes water associated with organic aerosol and inorganic aerosol, which
800 were calculated using an empirical method and a thermodynamic model, respectively.
801 Inorganic LWC (W_i) was predicted by ISORROPIA-II in forward mode in mol L^{-1} (Fountoukis
802 and Nenes, 2007). Inputs for ISORROPIA-II include inorganic aerosol mass concentrations

(${SO_4^{2-}}$, inorganic ${NO_3^-}$, and ammonium (${NH_4^+}$)) and meteorological parameters (temperature and RH). Calculation empirical of organic LWC (W_O) follows (Petters and Kreidenweis, 2007; Guo et al., 2015):

$$W_O = \frac{m_{org}\rho_w}{\rho_{org}} \frac{\kappa_{org}}{(1/RH - 1)} \quad (9)$$

where m_{org} is the organic mass concentration (μg m^{-3}), and ρ_w is the density of water (1 g cm^{-3}). The organic density (ρ_{org}, g cm^{-3}) was estimated using an empirical equation based on elemental ratios (Kuwata et al., 2012; Guo et al., 2015):

$$\rho_{org} = 1000 \times \left[\frac{12 + \frac{H}{C} + 16 \times \frac{O}{C}}{7.0 + 5 \times \frac{H}{C} + 4.15 \times \frac{O}{C}}\right] \quad (10)$$

The hygroscopicity of SOA generated during chamber studies under sub-saturated regimes depends on the OA degree of oxidation (Prenni et al., 2007; Jimenez et al., 2009; Petters et al., 2009; Chang et al., 2010). A simple linear relationship between the OA degree of oxidation (defined as the fraction of the total signal at *m/z* 44, f_{44}) and hygroscopicity (κ_{org}) is used (Duplissy et al., 2011):

$$\kappa_{org} = 2.2 \times f_{44} - 0.13 \quad (11)$$

The total LWC is then found by summing the water content associated with each mass fraction:

$$LWC = W_i + W_O \quad (12)$$

3 Results and Discussion

3.1 Temporal Dependences of Submicron Aerosol Composition

Campaign overview data for winter and summer are shown in Table 1 and Fig. 1~~,~~. This

includes~~ing~~ meteorological parameters (e.g., temperature, RH, radiometer, precipitation, wind direction and speed), trace gases (e.g., CO, SO_2, ~~NO,~~ NO_2, and O_3), chemically resolved NR-PM_1 concentrations~~, OM/OC, and elemental ratios (H/C, O/C, N/C and S/C)~~. ~~Data also are shown in Table 1.~~

Data indicate that the average concentration of NR-PM_1 during winter campaign was 6.0 ± 3.7 μg m^{-3}, ranging from 0.5 to 14.8 μg m^{-3}. Mass loadings of NR-PM_1 at this measurement site are relatively smaller than a site near the HSC in winter 2015 (10.8 μg m^{-3} (Wallace et al., 2018)), perhaps suggesting a weaker industrial influence at the UHSL site.

The average concentration of NR-PM_1 during summer was 3.6 ± 1.7 μg m^{-3}, ranging from 0.3 to 13.7 μg m^{-3}. For comparison, a summer campaign in 2006 on an elevated building near downtown Houston showed an average NR-PM_1 concentration of approximately 11 μg m^{-3} (Cleveland et al., 2012). An elevated NR-PM_1 episode was observed from May 28-31 (Fig. 1(~~m~~i)), with high solar radiation and O_x (O_x = NO_2 + O_3) levels during the daytime, and high RH at night, resulting in OA becoming the largest fractional species, likely due to gas-phase photochemical production of SOA together with the nighttime increase of SOA associated with high RH, lowered boundary layer and cooler temperatures.

In winter, OA was the largest component of NR-PM_1, accounting for ~~45.5~~38 ± 13~~.3~~% on average of the total mass, followed by SO_4^{2-} (~~19.9~~23 ± 11~~.2~~%), NO_3^-~~,AN~~ (~~17.2~~23 ± 1~~0.8~~%), NH_4^+ (~~13.2~~15 ± 5~~.4~~%)~~,~~ ~~$NO_{3,ON}$ (3.4 ± 1.4%)~~ and Cl^- (~~0.9~~1 ± 0.2%) (Fig. 2). Primary OA (POA=HOA+BBOA+COA) was responsible for ~~59~~61~~.1~~ ± 19~~.2~~% of OA mass. Secondary species (SO_4^{2-}+NO_3^-+NH_4^++LO-OOA+MO-OOA) accounted for ~~72.3~~ 76 ± ~~18~~21~~.1~~% of NR-PM_1 mass, which is higher than that in winter in Seoul (Kim et al., 2017) and Beijing (Hu

批注 [f1]:

批注 [f2]:

et al., 2016). ~~The inorganic aerosols in the winter were mostly neutralized in the forms of NH_4^+ salts (e.g., $(NH_4)_2SO_4$, NH_4NO_3, NH_4Cl) based on the predicted-to-measured NH_4^+ ratio of ~1 with correlation coefficient (r^2) of 0.98 (Fig. 3(A)).~~

In contrast to winter, OA during the summer campaign constituted on average ~~54.6~~47 ± 18~~.2~~% of NR-PM_1 mass, and SO_4^{2-} was the second largest component (~~30.9~~36 ± 15~~.5~~%), followed by NH_4^+ (1~~42.2~~ ± 5~~.2~~%). NO_3^-~~,ON and $NO_{3,AN}$~~ only accounted for ~~1.5~~2 ± 1~~.9~~% ~~and 0.4 ± 0.8%~~ of NR-PM_1 mass in the summer, respectively. Cl^- contributed ~~0.4~~1 ± 0.5% of NR-PM_1 mass. The increased PBL height in summer (Haman et al., 2012) likely contributed to relatively lower trace gas and NR-PM_1 levels in the summer. Secondary species contributed ~~~87.3~~88 ± ~~14.2~~15% of NR-PM_1 mass, indicating that the relative importance of secondary aerosol formation increased during summer as compared to winter, especially for species such as SO_4^{2-} and MO-OOA.

The total OA displayed high values during the nighttime hours in both winter and summer, maintaining a high level until morning rush hour, and then decreasing to a minimum value after 9:00 (Fig. ~~4~~3). The summertime OA presented a small peak at noon, suggesting that photochemical formation of OA played a more important role in summer than in winter. Increasing of ambient temperature and PBL height after sunrise causes re-partitioning to the gas phase, likely contributing to the decrease of OA, LO-OOA and ON during daytime.

Contributions of PMF factors to wintertime and summertime OA show significant differences. For wintertime OA, on average, BBOA, MO-OOA, and COA made similar contributions of ~~24~~26%, ~~23~~22% and 22% to total OA mass, respectively. The LO-OOA accounted for ~~18~~17% of OA mass, followed by HOA (13%). The POA constituted more than

批注 [f3]:

half of OA mass (~~59~~61%), with the remainder of being OOA (~~41~~39%). In the summer, LO-OOA represented the largest fraction of the OA mass (~~53~~54% on average), followed by MO-OOA (~~24~~23%), HOA (~~12~~15%) and BBOA (~~11~~8%). In the case of summer, OOA constituted 77% of OA and ~~42~~36% of total NR-PM_1 mass, which are almost two times their relative contributions in winter. The time series of mass concentrations of NR-PM_1 species (Fig. 1) and OA factors (Fig. ~~5~~4) in summer were relatively stable and repeatable, while it changed dramatically in winter due to the different meteorological conditions.

3.2 Seasonal Variation of the Formation of Sulfate and Nitrate

During the summer campaign, the prevailing southerly winds from the Gulf of Mexico carry marine aerosols to Houston (Schulze et al., 2018), resulting in a relatively high fraction of SO_4^{2-} and MSA. As shown in Fig. 1(~~m~~g, j), the increased contribution of SO_4^{2-} occurred when winds originated from the south at a high speed (e.g., May 16-27), while the contribution of SO_4^{2-} decreased significantly when winds originated from the north (e.g., May 10th and May 13-15). MSA ~~and S/C were~~ markedly elevated during periods of southerly winds (Fig. S~~1~~2(~~e,~~ ~~p~~F)), and O/C and OM/OC were relatively higher (Fig. ~~1~~S2(~~n~~D)). In addition, elevated SO_2 plumes were recorded during periods of southerly winds (Fig. 1(~~j~~g, h~~k~~)), potentially as a result of emissions from the Parish coal-fired power plant. In contrast to SO_4^{2-}, the fractional contribution of NO_3^- and OA increased greatly when the winds were not southerly. Primary pollutants such as CO~~, NO~~ and NO_2, were elevated when winds were northerly (Fig. 1(~~k~~h)), accompanied by lower O/C and higher H/C ratios during the corresponding periods (Fig. S2~~1~~(~~n~~D), e.g., May 1st, 2rd, 10th, 15th).

Diurnal patterns of NR-PM_1 and other species in the winter and summer (Fig. ~~4~~3) suggest

带格式的: 上标

889 significant seasonal dependence of sources and formation processes of NR-PM_1 species in
890 Houston. In the case of SO_4^{2-}, the diurnal pattern displayed a daytime peak in both winter and
891 summer, with the peak much more pronounced in summer mid-day. In winter, the f_{SO4} (mole
892 ratio of [SO_4^{2-}] to the sum of [SO_2] and [SO_4^{2-}]) and LWC have concurrent peak value during
893 the night time. However, there is no obvious correlation between f_{SO4} and LWC in summer,
894 though a moderate correlation (r = 0.44) was found in winter ~~(Fig. 3)~~. These results suggest that
895 SO_4^{2-} formed though aqueous-phase chemistry in winter is more prominent than that in
896 summer.

897 The total nitrate concentration was higher in winter than in summer. NO_3^-,AN was very low
898 in summer due to its thermal instability under high temperature, while it was relatively
899 enhanced in winter. According to the NO_x^+ ratio method described in Sec. 2.3.1, the mass
900 fraction of NO_3^-,AN in total nitrate was ~~decreased~~ in the range of 65-66~~from 90~~% ~~(1.26 μg m^{-3})~~
901 in winter, and in the range of 19-39~~ to 48~~% ~~(0.04 μg m^{-3})~~ in summer. The averaged bound
902 concentrations of NO_3,ON was ranged from 0.22-0.34~~14~~ μg m^{-3} in winter, and 0.05-0.06~~which is~~
903 ~~3.5 times that~~ μg m^{-3} in summer. The seasonal variation of NO_3^-,AN is much stronger than that
904 of NO_3,ON. This is in accordance with previous observations in Atlanta, Georgia and Centreville,
905 Alabama (Xu et al., 2015).

906 The diurnal profiles of NO_3,ON show that it reached peak value before dawn in both seasons
907 (Fig. ~~6~~5). However, NO_3^-,AN presents a bimodal diurnal profile in both seasons. The NO_3^-,AN,
908 which increased from late afternoon and peaked at 2:00-4:00, was likely formed through
909 nighttime chemistry from dinitrogen pentoxide (N_2O_5) hydrolysis, as the LWC displayed a
910 trend similar to that of NO_3^-,AN, This was corroborated by the observation of O_x (>25 ppb),

which is needed to form N_2O_5 (via $NO_3^{\cdot}$). The second peak observed during morning rush hour was likely formed though photochemical processing of NO_x emitted from vehicles because the traffic flow and O_x level are elevated during morning rush hour. The decreasing trend of $NO_{3,AN}^{-}$ after 9:00 is presumed to be a result of enhanced PBL height and evaporation.

The estimated ON accounted for ~~1 to 57~~4-8% of the total NR-PM_1 and ~~1 to 99~~9-17% percent of the OA ~~with an average contribution of about 12 and 37% to both~~in summer, 12-27% of the total NR-PM_1 and 31-66% percent of the OA in winter, which are comparable to other studies (Fry et al., 2009; Rollins et al., 2010; Xu et al., 2015; Berkemeier et al., 2016). ~~In winter, ON, on average accounted for 35 and 15% of NR-PM_1 and OA mass, respectively. Figure S3 presents a high ON loading period observed in summer.~~

A proxy for $NO_3^{\cdot}$ production rate is based on the product of the observations of [NO_2] and [O_3] (Rollins et al., 2012), where brackets represent mixing ratios in ppb. The O_x (> 25 ppb) and elevated NO_x observed at night in summer (Fig. ~~4~~3) resulted in rapid $NO_3^{\cdot}$ formation. Thus, the concurrent enhancement in ON and O_3 times NO_2 occurring during nighttime (Fig. S3) presumably was caused by the nocturnal $NO_3^{\cdot}$-initiated oxidation of anthropogenic and biogenic VOCs, with the latter probably larger than the former (Brown et al., 2013). The high N/C ratio of LO-OOA, concurrent peak value in LO-OOA and ON (MW=231 g mol^{-1}) during nighttime hours (Fig. ~~4~~3), and appreciable correlation of LO-OOA and ON ~~–~~in summer (r = 0.73) (Fig. ~~5~~4) together suggest that particle-phase ON from $NO_3^{\cdot}$-initiated chemistry contributed to nighttime LO-OOA in summer.

带格式的: 下标

带格式的: 上标

3.3 Effects of Aqueous-phase and Photochemical Oxidation on OOA Formation

On average, OOA accounted for ~~41~~ 39 ± 19% of OA mass in winter but increased to 77 ± 16% in summer. Note that MO-OOA accounted for more than half of OOA in winter (56%), indicating the more important role of MO-OOA in winter as compared to LO-OOA on a relative basis. In contrast, LO-OOA dominated OOA in summer (~~69~~70%). The mass spectra of MO-OOA in winter and summer are similar (Fig. ~~7~~6, r = 0.84) as are the extent of oxidation (O/C = 1.10 versus 1.07). However, LO-OOA in winter showed a different spectral pattern compared with that in summer. The mass spectrum of LO-OOA in winter was characterized by high *m/z* 32 (mainly CH_4O^+) and 46 (mainly $CH_2O_2^+$) peaks, resulting in a relatively high O/C (0.89) in winter that suggest LO-OOA in winter was more aged than that in summer (O/C=0.74).

Sun et al. (2016) reported a unique OOA in ambient air, termed aq-OOA (aqueous-phase-processed SOA), that strongly correlated with particle LWC, sulfate and S-containing ions. As shown in Table 2, by comparing the mass spectra of OOA in this work with aq-OOA, it is found that the mass spectra of MO-OOA in winter in this study presents a much stronger correlation (r =0.96) with aq-OOA, rather than LO-OOA in winter in this study (r =0.75). Both MO-OOA and LO-OOA in summer highly correlated with aq-OOA. This result indicates that the formation of LO-OOA in summer and MO-OOA in both seasons may involve aqueous-phase chemistry.

Assuming that OOA deduced from PMF analysis can be used as a surrogate of SOA (Wood et al., 2010; Xu et al., 2017), the two OOA were used to investigate the formation mechanisms and evolutionary processes of SOA. Previous studies have found SOA correlated well with odd oxygen (O_x) in many cities (Wood et al., 2010; Sun et al., 2011; Hayes et al., 2013; Zhang et al.,

2015; Xu et al., 2017) and that SOA formation is significantly impacted by aqueous-phase processing (Lim et al., 2010; Ervens et al., 2011; Xu et al., 2017). The relationships between OOA factors and O_x/LWC were used as the metrics to characterize SOA formation mechanisms associated with photochemistry/aqueous oxidation chemistry (Xu et al., 2017).

Fig. ~~8~~ 7 (A, B) indicates the LWC frequency distribution. Winter LWC are binned in 5 μg m^{-3} increments from 0 to 20 μg m^{-3}. Data in the ranges of 20 to 30 μg m^{-3}, 30 to 50 μg m^{-3}, 50 to 80 μg m^{-3}, and 80 to 120 μg m^{-3} are shown as 25, 40, 65 and 100 μg m^{-3}, respectively. Summer LWC are binned in 2.5 μg m^{-3} increments from 0 to 15 μg m^{-3}. The bins shown as 17.5 and 27.5 μg m^{-3} represent data from 15 to 20 μg m^{-3} and 20 to 35 μg m^{-3}. It should be noted that a fit for the binned data likely results in an increase in R^2 compared to the fit for the original data.

带格式的: 上标

The data associated with the artificially created bins in both seasons did not pass the normal test and homogeneity test of variances. The statistical significance of differences between bins was then tested using the Kruskal-Wallis analysis of variance (K-W ANOVA). The differences between winter and summer data of the bins were significant. Thus, the Dunn-Bonferroni test was performed for the *post-hoc* pairwise comparisons. It was found that the difference of all measured variables in different bins shown in Fig. 8 were significant (p<0.01). The results can be found in Tables ~~S5~~S6-~~S6~~S7. Fig. ~~8~~7(C, D) presents a clear positive trend of RH as a function of LWC in both winter and summer which implies an increased potential for aqueous-phase processing at high RH level, enhanced by low wind speed that allows accumulation of pollutants (Fig. ~~8~~7(E, F)). The patterns of other parameters as LWC increases in winter were different from those in summer.

The variation of binned mean OA mass against LWC presents significant seasonal difference (Fig. ~~8~~7(A, B)). In winter, the OA mass increased when LWC increased from 2.5 to 12.5 μg m^{-3} but decreased as the LWC increased further. The LO-OOA mass decreased dramatically when LWC>12.5 μg m^{-3} (RH>80%, Fig. ~~8~~7(C)) while MO-OOA continues increasing until LWC> 40 μg m^{-3}. This result indicates that wet removal may dominate under an extremely high RH environment coupled with stagnant air (WS <2 m/s Fig. ~~8~~7(E)), as the OA concentration decreased at extremely high LWC level (Fig. 7(A)). In summer, the OA mass decreased when LWC increased from 1.25 to 6.25 μg m^{-3} but increased when LWC increased further, suggesting the wet removal effect is not as strong as that in winter because of the relatively lower LWC in summer than in winter.~~,~~

On average, LO-OOA (Fig. ~~8~~7(G, H)) in winter increased from 0.3 to 0.9 μg m^{-3} when LWC increased from 2.5 to 7.5 μg m^{-3} but decreased as the LWC increased further, particularly when LWC >40 μg m^{-3}. The slope of this decrease was approximately -0.008 μg LO-OOA μg^{-1} LWC. Fig. ~~8~~7(A) shows that 64% of the data points were observed in the situation of low LWC (<12.5 μg m^{-3}, RH<80%), when the increase of LO-OOA was more significant than that of MO-OOA. In contrast, LO-OOA in summer showed a decreased trend under low LWC level (LWC<6.25 μg m^{-3}, RH<80%) but a significant linear increase from approximately 0.77 μm^{-3} to 1.8 μg m^{-3} as LWC increased from 6.25 to 27.5 μg m^{-3}, a slope of 0.053 μg LO-OOA μg^{-1} LWC. The relatively high LO-OOA under low LWC level was likely more regional, with contributions from possibly transported non-aqueous OOA, as the wind speed in this case was relatively high and RH was low. The formation of LO-OOA under high LWC level was likely enhanced by local aqueous-phase heterogeneous chemistry.

MO-OOA (Fig. ~~8~~7(I, J)) slightly increased during both seasons as LWC increased. In winter, MO-OOA presented a similar linear ~~increase~~ increasing trend from 0.57 to 0.98 μg m^{-3} when LWC increased from 2.5 to 40 μg m^{-3} but decreased as the LWC increased further ~~(probably due to the wet removal effect)~~. The slope of this increase was approximately 0.008 μg MO-OOA μg^{-1} LWC. In summer, MO-OOA appears to increase from 0.49 to 0.64 μg m^{-3} when LWC increased from 2.5 to 27.5 μg m^{-3}, with slope of 0.005 μg MO-OOA μg^{-1} LWC. In winter, because of the decrease in LO-OOA with LWC, the relative fraction of MO-OOA increases as LWC increases.

The mutual effect of aqueous-phase and photochemistry on OOA formation prevents solely evaluating the role of the two processes. Sullivan et al. (2016) reported multiple lines of evidence for local aq-SOA formation observed in the Po Valley, Italy during times of increasing RH, which coincided with dark conditions. Thus, the daytime data were separated to examine the variation of OOA against O_x. The relationship between OOA and aqueous-phase chemistry was investigated further by excluding the daytime data, with the aim of diminishing the influence of photochemistry. To do so, nighttime and daytime were based on sunrise and sunset in Houston during the two campaigns (https://www.timeanddate.com/sun/usa/houston). On average, the day lengths are 11 h 10 min and 13 h 35 min for the campaigns in February and May, 2014, respectively.

The potential linear relationship between OOA and LWC for the nighttime data was investigated by fitting the data with locally weighted scatter plot smoothing algorithm (LOWESS, (Cleveland, 1981)). According to the LOWESS curves for the original nighttime data and the resampled data obtained by bootstrap method (Figs. S14-15), it is interpreted that

there is likely exist a linear relationship between LO-OOA and LWC for data points with LWC less than 20 μg m^{-3} and great than 6 μg m^{-3} for the winter and summer campaign, respectively. As for MO-OOA, the linear relationship is likely exist when LWC less than 50 and 7 μg m^{-3} for the winter and summer campaign, respectively. ~~The~~

Figure ~~9~~8 presents the scatter plots of OOA versus LWC during nighttime for the two campaigns. The green dots denote the increasing trend of OOA against LWC. It is found that the increase of wintertime LO-OOA under low LWC level (<20 μg m^{-3}) during the night is stronger than that shown in Fig. ~~8~~ 7 (G). The nighttime LO-OOA linearly increased from 0.04 to 0.64 μg m^{-3} when LWC increased from 2.5 to 17.5 μg m^{-3}, a slope of 0.033 μg LO-OOA μg^{-1} LWC. This result indicates that the nighttime increase in LO-OOA in winter is more likely formed via aqueous-phase chemistry in aerosol liquid water. In contrast, the increase of LO-OOA under high LWC level (LWC>6.25 μg m^{-3}) in summer was less enhanced during nighttime (0.055 μg LO-OOA μg^{-1} LWC) as compared to the increase rate of whole dataset (0.053 μg LO-OOA μg^{-1} LWC). The slope of nighttime increase of MO-OOA against LWC during the winter campaign was 0.013 μg MO-OOA μg^{-1} LWC, which is 1.7 times the slope for the whole dataset (daytime and nighttime). For the summer campaign, the increase of nighttime MO-OOA is 2.2 times the rate for the whole dataset.

These results suggest that aqueous-phase processing likely has a strong positive impact on the formation of MO-OOA in the two seasons except for instances when LWC exceeds 100 μg m^{-3} in winter. It also appears to facilitate the local formation of LO-OOA under low LWC level (<17.5 μg m^{-3}) in winter and under relatively high LWC level (>6.25 μg m^{-3}) in summer.

As mentioned previously, ON contributes significantly to summertime LO-OOA, and the

带格式的: 上标

concurrent enhancement in ON (MW=231 g mol^{-1}) and LO-OOA during night was associated with elevated RH (Fig. 43). A previous study found that the partitioning of organic compounds to the particle phase was significantly increased at elevated RH levels (70%) in an urban area dominated by biogenic emissions in Atlanta (Hennigan et al., 2008). The correlation of ON and LO-OOA in summer nighttime (r=0.76) was stronger than that during daytime (r =0.53). Thus, we presume that aerosol water facilitates the formation of ON from NO_3˙-initiated chemistry involving BVOCs during nighttime, resulting in a good relationship of LO-OOA and LWC in summer.

MSA is a secondary product from the oxidation of dimethyl sulfide ~~(DMS)~~ (Zorn et al., 2008), which is a gaseous species emission from marine organisms (Barnes et al., 2006). Thus, MSA is found to be abundant in marine/coastal areas and play an important role in the formation of marine PM (Gondwe, et al., 2004; Huang et al., 2015; Schulze et al., 2018). The formation of MSA is unique to aqueous-phase processing, and could be used as an indicator of aqueous SOA formation (Barnes et al., 2006; Ervens et al., 2011). Recent observations confirmed that MSA and associated fragment ions ($CH_2O_2^+$ (m/z 46), $C_2O_2^+$ (m/z 56) and $C_2H_2O_2^+$ (m/z 58), which are unique ions of glyoxal and methylglyoxal uptake on SOA (Chhabra et al., 2010)) strongly correlated with SOA formed via aqueous-phase processing (Ge et al., 2012; Sun et al., 2016). In this work, the MO-OOA formation was associated with aqueous-phase oxidation more strongly than LO-OOA in winter, which likely can be further verified by the correlations between MO-OOA/LO-OOA and MSA. As shown in Fig. 76, MSA has a relatively higher correlation coefficient with MO-OOA (r=0.45) compared to LO-OOA (r=0.30), though the correlation also is influenced by many other factors.

带格式的: 上标

Fig. ~~10~~ 9(A, B) presents the frequency distribution of O_x. Winter O_x are binned in 10 ppb increments from 0 to 60 ppb. The range for summer is 20 to 70 ppb. The data associated with the artificially created O_x bins in both seasons did not pass the normal test and homogeneity test of variances. The K-W ANOVA for winter and summer data of the bins were significant. The Dunn-Bonferroni test for the *post-hoc* pairwise comparisons shows that the difference of measured variables among different bins shown in Fig. ~~10~~ 9 were significant (Tables ~~S7~~S8-S~~8~~9). The clear positive relationship between solar radiation and O_x is shown in Fig. ~~10~~ 9 (C, D), and the negative relationship between solar radiation and RH is shown in Fig. ~~10~~ 9 (E, F), suggesting strong atmospheric photochemical activity associated with high O_x periods.

The variations of LO-OOA and MO-OOA showed substantially different patterns with increases of O_x in winter and summer. In winter, LO-OOA and MO-OOA showed comparable increasing trends at low O_x level (<35 ppb), with MO-OOA having a stronger response. The LO-OOA was increased from 0.13 to 0.72 μg m^{-3} when O_x increased from 5 to 35 ppb but decreased as the O_x increased further. The slope of this increase was approximately 0.023 μg LO-OOA ppb^{-1} O_x. MO-OOA increased from 0.13 to 0.88 μg m^{-3} when the O_x increased from 5 to 35 ppb, with a slope of 0.027 μg MO-OOA ppb^{-1} O_x. This leads to a maximum in the mass fraction of MO-OOA in the mid-O_x level range and also at highest levels of observed O_x.

In summer, there is a clear decreasing trend of RH with increases of O_x. As discussed previously, the high level of summertime LO-OOA likely was associated with high LWC. Therefore, the high mass fraction of LO-OOA at the lowest O_x level (<20 ppb) associated with the high RH/LWC was likely from aqueous-phase chemistry. After excluding ~~low~~ low-O_x data (<20 ppb), LO-OOA showed a much stronger response to O_x than did MO-OOA. The summer

LO-OOA showed a significant linear increase from approximately 0.6 to 1.8 μg m^{-3} when O_x increased from 25 to 65 ppb, a slope of 0.03 μg LO-OOA ppb^{-1} O_x. This increase was likely in the case of low RH conditions (<80%, Fig. ~~8~~ 7 (D)), when aqueous-phase chemistry did not promote the formation of LO-OOA (Fig. ~~8~~ 7 (H)). Summer MO-OOA increased from 0.36 to 0.67 μg m^{-3} when O_x increased from 25 to 55 ppb but decreased as the O_x increased further. The slope of this increase was 0.007 μg MO-OOA ppb^{-1} O_x. Contrary to winter, LO-OOA responded more strongly to increases of O_x than MO-OOA did.

The relationship of OOA versus O_x was examined further by excluding nighttime data. According to the LOWESS curves for the original daytime data and resampled data obtained using bootstrap method (Figs.S16-17), it is interpreted that there is likely exist a linear relationship between LO-OOA and O_x when O_x less than 35 ppb and great than 20 ppb for the winter and summer period, respectively. As for MO-OOA, the linear relationship likely exists for data points with Ox less than 35 ppb for the winter period, but it is less prominent.

Figure ~~11~~ 10 presents the scatter plots of daytime OOA versus O_x for the winter and summer campaign. The daytime responses of LO-OOA and MO-OOA to O_x in winter were ~1.5 times that for the whole dataset (Fig. ~~10~~ 9 (G, I)), and the increase rate of MO-OOA was higher than that of LO-OOA. In summer, the slope of the daytime increase of LO-OOA was 1.24 times that for the whole campaign (Fig. 10 (H))~~, and the increase rate of daytime MO-OOA was close to that for whole dataset~~. These results suggest that the photochemical enhancement of OOA in winter was more prominent than that in summer. For the summer campaign, the formation of LO-OOA was more strongly linked to photochemistry compared to MO-OOA. At low atmospheric oxidative capacity (Ox<20 ppb), aqueous-phase chemistry was

带格式的: 下标

带格式的: 下标

likely predominant in the formation of LO-OOA.

The combined effects of photochemistry and aqueous-phase chemistry on OOA composition during winter and summer are further demonstrated in Fig. ~~12~~11. The ratio of MO-OOA/LO-OOA in winter showed the highest values on the left-top corner in Fig. ~~12~~ 11 (A), suggesting photochemical processing was likely responsible for MO-OOA formation, under low LWC levels (< 10 μg m^{-3}). Additionally, data with high MO-OOA/LO-OOA on the right-bottom corner in Fig. ~~12~~ 11 (A) indicate the important role of aqueous-phase chemistry under low O_x and high LWC levels. Overall, the concentration of MO-OOA in winter increased as O_x/LWC increased, whereas LO-OOA markedly decreased. This result indicates both photochemical and aqueous-phase processing played a more important role in enhancing MO-OOA than LO-OOA in winter. Furthermore, the diurnal patterns of wintertime LO-OOA only presented a peak value at night while MO-OOA showed one peak value at night (high LWC) and another one in the afternoon (high O_x period) (Fig. ~~4~~3).

In summer, data points with low MO-OOA/LO-OOA value on the left-top of Figure ~~12~~ 11 (B) illustrated that LO-OOA was enhanced in high-O_x and low-LWC condition, though the low MO-OOA/LO-OOA are not confined to just the top left. In case of high LWC level (LWC> 6.5 μg m^{-3}), MO-OOA/LO-OOA were much lower (on the right of Figure ~~12~~ 11 (B), particularly when LWC> 10 μg m^{-3}). Although MO-OOA increased with LWC and O_x, the increase of LO-OOA was more significant. The effects of both photochemistry (≥ 25 ppb) and aqueous-phase chemistry (≥ 6.5 μg m^{-3}) were more relevant for the formation of LO-OOA than MO-OOA. On average, the mass concentration of LO-OOA was elevated by nearly 1.2 μg m^{-3} as a ~20 μg change in LWC (increased from 6.25 μg m^{-3} to 27.5 μg m^{-3}, Fig. ~~8~~ 7 (H)), which is

equivalent to a 40 ppb change in O_x (increased from 25 ppb to 65 ppb, Fig. ~~10~~ 9 (H)). This result further suggests that the aqueous-phase chemistry is comparable to photochemistry in processing LO-OOA in summer. The diurnal pattern of summertime LO-OOA displays a peak value at night and a comparable peak value in the afternoon (Fig. ~~4~~3).

4 Conclusions

Seasonal characterization of NR-PM_1 collected using HR-ToF-AMS near Houston in 2014 demonstrated that the mass loading, diurnal patterns, and important formation pathways of NR-PM_1 vary seasonally. The OA was the largest component of NR-PM_1 mass, on average, accounting for ~~46~~38% and ~~55~~47% of the mass loadings in winter and summer, respectively, which is less than that in the north part of Houston, which is influenced by high biogenic emission rates. ~~Inorganic~~ N~~n~~itrate was the second largest component in winter (~~17~~23%) but accounted for only ~~0.4~~2% of NR-PM_1 mass in summer; SO_4^{2-} was the ~~third and~~ second largest component in winter (~~20~~23%) and summer (~~31~~36%), respectively. ON, on average accounted for ~~15~~31-66 and ~~3~~9-17 % of OA during winter and summer campaign, respectively. The summertime ON correlated very well with LO-OOA and concurrently peaked at nighttime. It is likely that ON from $NO_3^{\bullet}$-initiated oxidation of BVOC in the forested northeastern Houston contributed greatly to nighttime LO-OOA in summer.

Contributions of factors to wintertime and summertime OA show distinct differences. For wintertime OA, on average, BBOA contributed 26% of OA mass, MO-OOA~~,~~ and COA made ~~similar~~ the same contributions of ~~24%, 23% and~~ 22% to total OA mass~~, respectively~~. LO-OOA accounted for ~~18~~17% of OA mass, followed by HOA (13%). In the summer, LO-OOA

represented the largest fraction of the OA mass, ~~53~~54% on average. The second largest contributor was MO-OOA (~~24~~23%). Together, POA constituted more than half of OA mass (~~59~~61%) in winter, while it accounted for 23% of OA mass in summer, highlighting the enhanced impact of primary emissions on OA level during wintertime. Secondary aerosols account for ~76% and ~~89~~88% of NR-PM_1 mass in winter and summer, respectively, indicating NR-PM_1 mass was likely driven mostly by secondary aerosol formation.

The two proxies of SOA (LO-OOA and MO-OOA) presented seasonal differences in their spectral patterns, oxidation degrees and contributions to SOA. MO-OOA showed a higher contribution to SOA than LO-OOA in winter (56% vs. 44%). In contrast, LO-OOA dominated SOA in summer (~~69~~70%). Our results indicate that both photochemical and aqueous-phase chemistry played important roles in the formation of MO-OOA and LO-OOA. Aqueous-phase processing likely has strong positive impact on the formation of MO-OOA in the two seasons, especially in winter. The relationships between MO-OOA and LWC were 0.~~0076~~ 008 and 0.00~~4~~5 μg MO-OOA μg^{-1} LWC during winter and summer, respectively. Wet removal likely limits MO-OOA when LWC exceeds 100 μg m^{-3} in winter. ~~Interestingly, t~~The relative importance of aqueous-phase chemistry versus photochemistry in processing LO-OOA was dependent on RH. Aqueous-phase processing likely facilitated the local formation of wintertime LO-OOA at low LWC level (<17.5 μg m^{-3}, RH<80%), with a stronger dependence (0.033 μg LO-OOA μg^{-1} LWC) than MO-OOA. In summer, the formation of LO-OOA was enhanced by aqueous-phase processing at relatively high LWC level (>6.25 μg m^{-3}, RH>80%) with a slope of 0.~~0526~~ 053 μg LO-OOA μg^{-1} LWC, while LO-OOA was likely transported non-aqueous regional OOA when LWC < 6.25 μg m^{-3}. These increases of OOA in response to

LWC were greatly enhanced during nighttime. Aqueous-phase chemistry also was predominant in the formation of summertime LO-OOA at low atmospheric oxidative capacity (O_x < 20 ppb). In general, summertime LO-OOA showed a much stronger response to O_x than did MO-OOA, with a slope of 0.~~0299~~ 030 μg LO-OOA ppb^{-1} O_x. LO-OOA in summer was elevated by nearly 1.2 μg m^{-3} as a ~20 μg change in LWC, which is equivalent to a 40 ppb change in O_x.

Acknowledgments

The authors would like to acknowledge Yele Sun (Institute of Atmospheric Physics, Chinese Academy of Sciences) for providing the aq-OOA mass spectra, and Qiao Zhu (Peking University Shenzhen Graduate School) for assistance in the calculation of organic nitrates and PMF analysis. The scholarships provided by China Scholarship Council to Qili Dai and Xiaohui Bi are gratefully acknowledged. Support of the Houston Endowment in development and deployment of the MAQL also is gratefully acknowledged. Datasets are available by contacting the corresponding author.

Author contribution. Qili Dai performed the data analysis and wrote the manuscript. Robert J. Griffin and Yinchang Feng assisted heavily with manuscript development and editing. Henry W. Wallace, Alexander A.T. Bui, James H. Flynn, Barry L. Lefer contributed to data collection during the field campaigns. Benjamin C. Schulze, Henry W. Wallace, Alexander A.T. Bui and Nancy P. Sanchez contributed with data analysis. Xiaohui Bi, Benjamin C. Schulze, Alexander

A.T. Bui, Fangzhou Guo, Nancy P. Sanchez, James H. Flynn provided helpful comments and edits.

Competing interests. The authors declare that they have no conflict of interest.

References

Allen, D. T., and Fraser, M.: An overview of the Gulf Coast Aerosol Research and Characterization Study: The Houston Fine Particulate Matter Supersite, J. Air Waste Manage., 56, 456-466, http://doi.org/10.1080/10473289.2006.10464514, 2006.

Atkinson, D. B., Massoli, P., O'Neill, N. T., Quinn, P. K., Brooks, S. D., and Lefer, B.: Comparison of in situ and columnar aerosol spectral measurements during TexAQS-GoMACCS 2006: testing parameterizations for estimating aerosol fine mode properties, Atmos. Chem. Phys., 10, 51-61, http://doi.org/10.5194/acp-10-51-2010, 2010.

Ayres, B. R., Allen, H. M., Draper, D. C., Brown, S. S., Wild, R. J., Jimenez, J. L., Day, D. A., Campuzano-Jost, P., Hu, W., de Gouw, J., Koss, A., Cohen, R. C., Duffey, K. C., Romer, P., Baumann, K., Edgerton, E., Takahama, S., Thornton, J. A., Lee, B. H., Lopez-Hilfiker, F. D., Mohr, C., Wennberg, P. O., Nguyen, T. B., Teng, A., Goldstein, A. H., Olson, K., and Fry, J. L.: Organic nitrate aerosol formation via NO_3 + biogenic volatile organic compounds in the southeastern United States, Atmos. Chem. Phys., 15, 13377-13392, http://doi.org/10.5194/acp-15-13377-2015, 2015.

Bahreini, R., Ervens, B., Middlebrook, A. M., Warneke, C., de Gouw, J. A., DeCarlo, P. F., Jimenez, J. L., Brock, C. A., Neuman, J. A., Ryerson, T. B., Stark, H., Atlas, E., Brioude, J., Fried, A., Holloway, J. S., Peischl, J., Richter, D., Walega, J., Weibring, P., Wollny, A. G., and Fehsenfeld, F. C.: Organic aerosol formation in urban and industrial plumes near Houston and Dallas, Texas, J. Geophys. Res., 114, D00f16, http://doi.org/10.1029/2008jd011493, 2009.

Barnes, I., Hjorth, J., and Mihalopoulos, N.: Dimethyl sulfide and dimethyl sulfoxide and their oxidation in the atmosphere, Chem. Rev., 106, 940-975, http://doi.org/10.1021/cr020529+, 2006.

Bates, T. S., Quinn, P. K., Coffman, D., Schulz, K., Covert, D. S., Johnson, J. E., Williams, E. J., Lerner, B. M., Angevine, W. M., Tucker, S. C., Brewer, W. A., and Stohl, A.: Boundary layer aerosol chemistry during TexAQS/GoMACCS 2006: Insights into aerosol sources and transformation processes, J. Geophys. Res., 113, D00f01, http://doi.org/10.1029/2008jd010023, 2008.

Bean, J. K., Faxon, C. B., Leong, Y. J., Wallace, H. W., Cevik, B. K., Ortiz, S., Canagaratna, M. R., Usenko, S., Sheesley, R. J., Griffin, R. J., and Hildebrandt, L: Composition and sources of particulate matter measured near Houston, TX; Anthropogenic-biogenic interactions, Atmos., 7, 73, https://doi.org/10.3390/atmos7050073, 2016

Berkemeier, T., Ammann, M., Mentel, T. F., Poschl, U., and Shiraiwa, M.: Organic Nitrate Contribution to New Particle Formation and Growth in Secondary Organic Aerosols from alpha-Pinene Ozonolysis, Environ. Sci. Technol., 50, 6334-6342, http://doi.org/10.1021/acs.est.6b00961, 2016.

Boyd, C. M., Sanchez, J., Xu, L., Eugene, A. J., Nah, T., Tuet, W. Y., Guzman, M. I., and Ng, N. L.: Secondary Organic Aerosol (SOA) formation from the β-pinene CNO3 system: effect of humidity and peroxy radical fate, Atmos. Chem. Phys., 15, 7497–7522, doi:10.5194/acp-15-7497-2015, 2015.

Brown, S. S., Dube, W. P., Bahreini, R., Middlebrook, A. M., Brock, C. A., Warneke, C., de Gouw, J. A., Washenfelder, R. A., Atlas, E., Peischl, J., Ryerson, T. B., Holloway, J. S., Schwarz, J. P., Spackman, R., Trainer, M., Parrish, D. D., Fehshenfeld, F. C., and Ravishankara, A. R.: Biogenic VOC oxidation and organic aerosol formation in an urban nocturnal boundary layer: aircraft vertical profiles in Houston, TX, Atmos. Chem. Phys., 13, 11317-11337, http://doi.org/10.5194/acp-13-11317-2013, 2013.

Bruns, E. A., Perraud, V., Zelenyuk, A., Ezell, M. J., Johnson, S. N., Yu, Y., Imre, D., Finlayson-Pitts, B. J., and Alexander, M. L.: Comparison of FTIR and Particle Mass Spectrometry for the Measurement of Particulate Organic Nitrates, Environ. Sci. Technol., 44, 1056–1061, 2010.

~~Budisulistiorini, S. H., Baumann, K., Edgerton, E. S., Bairai, S. T., Mueller, S., Shaw, S. L., Knipping, E. M., Gold, A., and Surratt, J. D.: Seasonal characterization of submicron aerosol chemical composition and organic aerosol sources in the southeastern United States: Atlanta, Georgia,and Look Rock, Tennessee, Atmos. Chem. Phys., 16, 5171-5189, http://doi.org/10.5194/acp-16-5171-2016, 2016.~~

Canagaratna, M. R., Jayne, J. T., Jimenez, J. L., Allan, J. D., Alfarra, M. R., Zhang, Q., Onasch, T. B., Drewnick, F., Coe, H., Middlebrook, A., Delia, A., Williams, L. R., Trimborn, A. M., Northway, M. J., DeCarlo, P. F., Kolb, C. E., Davidovits, P., and Worsnop, D. R.: Chemical

带格式的: 左, 3 级, 行距: 单倍行距, 到齐到网格

带格式的: 左, 3 级, 行距: 单倍行距, 到齐到网格

and microphysical characterization of ambient aerosols with the aerodyne aerosol mass spectrometer, Mass Spectrom. Rev., 26, 185-222, http://doi.org/10.1002/mas.20115, 2007.

Canagaratna, M. R., Jimenez, J. L., Kroll, J. H., Chen, Q., Kessler, S. H., Massoli, P., Hildebrandt Ruiz, L., Fortner, E., Williams, L. R., Wilson, K. R., Surratt, J. D., Donahue, N. M., Jayne, J. T., and Worsnop, D. R.: Elemental ratio measurements of organic compounds using aerosol mass spectrometry: characterization, improved calibration, and implications, Atmos. Chem. Phys., 15, 253-272, http://doi.org/10.5194/acp-15-253-2015, 2015.

~~Chakraborty, A., Bhattu, D., Gupta, T., Tripathi, S. N., and Canagaratna, M. R.: Real-time measurements of ambient aerosols in a polluted Indian city: Sources, characteristics, and processing of organic aerosols during foggy and nonfoggy periods, J. Geophys. Res., 120, 9006-9019, http://doi.org/10.1002/2015jd023419, 2015.~~

Chang, R. Y. W., Slowik, J. G., Shantz, N. C., Vlasenko, A., Liggio, J., Sjostedt, S. J., Leaitch, W. R., and Abbatt, J. P. D.: The hygroscopicity parameter (kappa) of ambient organic aerosol at a field site subject to biogenic and anthropogenic influences: relationship to degree of aerosol oxidation, Atmos. Chem. Phys., 10, 5047-5064, http://doi.org/10.5194/acp-10-5047-2010, 2010.

Chhabra, P. S., Flagan, R. C., and Seinfeld, J. H.: Elemental analysis of chamber organic aerosol using an aerodyne high-resolution aerosol mass spectrometer, Atmos. Chem. Phys., 10, 4111-4131, http://doi.org/10.5194/acp-10-4111-2010, 2010.

Cleveland, M. J., Ziemba, L. D., Griffin, R. J., Dibb, J. E., Anderson, C. H., Lefer, B., and Rappengluck, B.: Characterization of urban aerosol using aerosol mass spectrometry and proton nuclear magnetic resonance spectroscopy, Atmos. Environ., 54, 511-518, http://doi.org/10.1016/j.atmosenv.2012.02.074, 2012.

Cleveland, W. S. (1981) LOWESS: A program for smoothing scatterplots by robust locally weighted regression. Am. Stat., 35, 54.

Crippa, M., El Haddad, I., Slowik, J. G., DeCarlo, P. F., Mohr, C., Heringa, M. F., Chirico, R., Marchand, N., Sciare, J., Baltensperger, U., and Prevot, A. S. H.: Identification of marine and continental aerosol sources in Paris using high resolution aerosol mass spectrometry, J. Geophys. Res., 118, 1950-1963, http://doi.org/10.1002/jgrd.50151, 2013a.

~~Crippa, M., DeCarlo, P. F., Slowik, J. G., Mohr, C., Heringa, M. F., Chirico, R., Poulain, L., Freutel, F., Sciare, J., Cozic, J., Di Marco, C. F., Elsasser, M., Nicolas, J. B., Marchand, N., Abidi, E., Wiedensohler, A., Drewnick, F., Schneider, J., Borrmann, S., Nemitz, E., Zimmermann, R., Jaffrezo, J. L., Prevot, A. S. H., and Baltensperger, U.: Wintertime~~

~~aerosol chemical composition and source apportionment of the organic fraction in the metropolitan area of Paris, Atmos. Chem. Phys., 13, 961-981, http://doi.org/10.5194/acp-13-961-2013, 2013b.~~

~~de Gouw, J. A., Brock, C. A., Atlas, E. L., Bates, T. S., Fehsenfeld, F. C., Goldan, P. D., Holloway, J. S., Kuster, W. C., Lerner, B. M., Matthew, B. M., Middlebrook, A. M., Onasch, T. B., Peltier, R. E., Quinn, P. K., Senff, C. J., Stohl, A., Sullivan, A. P., Trainer, M., Warneke, C., Weber, R. J., and Williams, E. J.: Sources of particulate matter in the northeastern United States in summer: 1. Direct emissions and secondary formation of organic matter in urban plumes, J. Geophys. Res., 113, D08301, http://doi.org/10.1029/2007jd009243, 2008.~~

DeCarlo, P. F., Kimmel, J. R., Trimborn, A., Northway, M. J., Jayne, J. T., Aiken, A. C., Gonin, M., Fuhrer, K., Horvath, T., Docherty, K. S., Worsnop, D. R., and Jimenez, J. L.: Field-deployable, high-resolution, time-of-flight aerosol mass spectrometer, Anal. Chem., 78, 8281-8289, http://doi.org/10.1021/ac061249n, 2006.

Duplissy, J., DeCarlo, P. F., Dommen, J., Alfarra, M. R., Metzger, A., Barmpadimos, I., Prevot, A. S. H., Weingartner, E., Tritscher, T., Gysel, M., Aiken, A. C., Jimenez, J. L., Canagaratna, M. R., Worsnop, D. R., Collins, D. R., Tomlinson, J., and Baltensperger, U.: Relating hygroscopicity and composition of organic aerosol particulate matter, Atmos. Chem. Phys., 11, 1155-1165, http://doi.org/10.5194/acp-11-1155-2011, 2011.

El-Sayed, M. M. H., Amenumey, D., and Hennigan, C. J.: Drying-Induced Evaporation of Secondary Organic Aerosol during Summer, Environ Sci Technol, 50, 3626-3633, 10.1021/acs.est.5b06002, 2016.

Ervens, B., Turpin, B. J., and Weber, R. J.: Secondary organic aerosol formation in cloud droplets and aqueous particles (aqSOA): a review of laboratory, field and model studies, Atmos. Chem. Phys., 11, 11069-11102, http://doi.org/10.5194/acp-11-11069-2011, 2011.

Farmer, D. K., Matsunaga, A., Docherty, K. S., Surratt, J. D., Seinfeld, J. H., Ziemann, P. J., and Jimenez, J. L.: Response of an aerosol mass spectrometer to organonitrates and organosulfates and implications for atmospheric chemistry, P. Natl. Acad. Sci. USA, 107, 6670-6675, http://doi.org/10.1073/pnas.0912340107, 2010.

Fountoukis, C., and Nenes, A.: ISORROPIA II: a computationally efficient thermodynamic equilibrium model for K+-Ca2+-Mg2+-Nh(4)(+)-Na+-SO42--NO3--Cl--H2O aerosols, Atmos. Chem. Phys., 7, 4639-4659, , http://doi.org/10.5194/acp-7-4639-2007, 2007.

Fry, J. L., Kiendler-Scharr, A., Rollins, A. W., Wooldridge, P. J., Brown, S. S., Fuchs, H., Dube, W., Mensah, A., dal Maso, M., Tillmann, R., Dorn, H. P., Brauers, T., and Cohen, R. C.:

带格式的: 左, 行距: 单倍行距, 到齐到网格

Organic nitrate and secondary organic aerosol yield from NO3 oxidation of beta-pinene evaluated using a gas-phase kinetics/aerosol partitioning model, Atmos. Chem. Phys., 9, 1431-1449, http://doi.org/10.5194/acp-9-1431-2009, 2009.

Fry, J. L., Draper, D. C., Zarzana, K. J., Campuzano-Jost, P., Day, D. A., Jimenez, J. L., Brown, S. S., Cohen, R. C., Kaser, L., Hansel, A., Cappellin, L., Karl, T., Roux, A. H., Turnipseed, A., Cantrell, C., Lefer, B. L., and Grossberg, N.: Observations of gas- and aerosol-phase organic nitrates at BEACHON-RoMBAS 2011, Atmos. Chem. Phys., 13, 8585-8605, http://doi.org/10.5194/acp-13-8585-2013, 2013.

Ge, X., Zhang, Q., Sun, Y., Ruehl, C. R., and Setyan, A.: Effect of aqueous-phase processing on aerosol chemistry and size distributions in Fresno, California, during wintertime, Environ. Chem., 9, 221, http://doi.org/10.1071/en11168, 2012.

Gondwe, M., Krol, M., Klaassen, W., Gieskes, W., and de Baar, H.: Comparison of modeled versus measured MSA:nss SO4= ratios: A global analysis, Global Biogeochem. Cy., 18, http://doi.org/10.1029/2003GB002144, 2004.

Grantz, D. A., Garner, J. H. B., and Johnson, D. W.: Ecological effects of particulate matter, Environ. Int., 29, 213-239, http://doi.org/10.1016/S0160-4120(02)00181-2, 2003.

Guo, H., Xu, L., Bougiatioti, A., Cerully, K. M., Capps, S. L., Hite, J. R., Carlton, A. G., Lee, S. H., Bergin, M. H., Ng, N. L., Nenes, A., and Weber, R. J.: Fine-particle water and pH in the southeastern United States, Atmos. Chem. Phys., 15, 5211-5228, http://doi.org/10.5194/acp-15-5211-2015, 2015.

Haman, C. L., Lefer, B., and Morris, G. A.: Seasonal Variability in the Diurnal Evolution of the Boundary Layer in a Near-Coastal Urban Environment, J. Atmos. Ocean Tech., 29, 697-710, , http://doi.org/10.1175/Jtech-D-11-00114.1, 2012.

Hayes, P. L., Ortega, A. M., Cubison, M. J., Froyd, K. D., Zhao, Y., Cliff, S. S., Hu, W. W., Toohey, D. W., Flynn, J. H., Lefer, B. L., Grossberg, N., Alvarez, S., Rappenglueck, B., Taylor, J. W., Allan, J. D., Holloway, J. S., Gilman, J. B., Kuster, W. C., De Gouw, J. A., Massoli, P., Zhang, X., Liu, J., Weber, R. J., Corrigan, A. L., Russell, L. M., Isaacman, G., Worton, D. R., Kreisberg, N. M., Goldstein, A. H., Thalman, R., Waxman, E. M., Volkamer, R., Lin, Y. H., Surratt, J. D., Kleindienst, E., Offenberg, J. H., Dusanter, S., Griffith, S., Stevens, P. S., Brioude, J., Angevine, W. M., and Jimenez, J. L.: Organic aerosol composition and sources in Pasadena, California, during the 2010 CalNex campaign, J. Geophys. Res., 118, 9233-9257, http://doi.org/10.1002/jgrd.50530, 2013.

Hennigan, C. J., Bergin, M. H., Dibb, J. E., and Weber, R. J.: Enhanced secondary organic

aerosol formation due to water uptake by fine particles, Geophys. Res. Lett., 35, L18801, http://doi.org/10.1029/2008gl035046, 2008.

Hu, W. W., Campuzano-Jost, P., Palm, B. B., Day, D. A., Ortega, A. M., Hayes, P. L., Krechmer, J. E., Chen, Q., Kuwata, M., Liu, Y. J., de Sa, S. S., McKinney, K., Martin, S. T., Hu, M., Budisulistiorini, S. H., Riva, M., Surratt, J. D., St Clair, J. M., Isaacman-Van Wertz, G., Yee, L. D., Goldstein, A. H., Carbone, S., Brito, J., Artaxo, P., de Gouw, J. A., Koss, A., Wisthaler, A., Mikoviny, T., Karl, T., Kaser, L., Jud, W., Hansel, A., Docherty, K. S., Alexander, M. L., Robinson, N. H., Coe, H., Allan, J. D., Canagaratna, M. R., Paulot, F., and Jimenez, J. L.: Characterization of a real-time tracer for isoprene epoxydiols-derived secondary organic aerosol (IEPOX-SOA) from aerosol mass spectrometer measurements, Atmos. Chem. Phys., 15, 11807-11833, http://doi.org/10.5194/acp-15-11807-2015, 2015.

Hu, W. W., Hu, M., Hu, W., Jimenez, J. L., Yuan, B., Chen, W. T., Wang, M., Wu, Y. S., Chen, C., Wang, Z. B., Peng, J. F., Zeng, L. M., and Shao, M.: Chemical composition, sources, and aging process of submicron aerosols in Beijing: Contrast between summer and winter, J. Geophys. Res., 121, 1955-1977, http://doi.org/10.1002/2015jd024020, 2016.

Huang, D. D., Li, Y. J., Lee, B. P., and Chan, C. K.: Analysis of Organic Sulfur Compounds in Atmospheric Aerosols at the HKUST Supersite in Hong Kong using HR-ToF-AMS, Environ. Sci. Technol., 49, 3672-3679, http://doi.org/10.1021/es5056269, 2015.

Jimenez, J. L., Canagaratna, M. R., Donahue, N. M., Prevot, A. S. H., Zhang, Q., Kroll, J. H., DeCarlo, P. F., Allan, J. D., Coe, H., Ng, N. L., Aiken, A. C., Docherty, K. S., Ulbrich, I. M., Grieshop, A. P., Robinson, A. L., Duplissy, J., Smith, J. D., Wilson, K. R., Lanz, V. A., Hueglin, C., Sun, Y. L., Tian, J., Laaksonen, A., Raatikainen, T., Rautiainen, J., Vaattovaara, P., Ehn, M., Kulmala, M., Tomlinson, J. M., Collins, D. R., Cubison, M. J., Dunlea, E. J., Huffman, J. A., Onasch, T. B., Alfarra, M. R., Williams, P. I., Bower, K., Kondo, Y., Schneider, J., Drewnick, F., Borrmann, S., Weimer, S., Demerjian, K., Salcedo, D., Cottrell, L., Griffin, R., Takami, A., Miyoshi, T., Hatakeyama, S., Shimono, A., Sun, J. Y., Zhang, Y. M., Dzepina, K., Kimmel, J. R., Sueper, D., Jayne, J. T., Herndon, S. C., Trimborn, A. M., Williams, L. R., Wood, E. C., Middlebrook, A. M., Kolb, C. E., Baltensperger, U., and Worsnop, D. R.: Evolution of Organic Aerosols in the Atmosphere, Science, 326, 1525-1529, http://doi.org/10.1126/science.1180353, 2009.

Kim, H., Zhang, Q., Bae, G. N., Kim, J. Y., and Lee, S. B.: Sources and atmospheric processing of winter aerosols in Seoul, Korea: insights from real-time measurements using a high-resolution aerosol mass spectrometer, Atmos. Chem. Phys., 17, 2009-2033,

http://doi.org/10.5194/acp-17-2009-2017, 2017.

Kota, S. H., Park, C., Hale, M. C., Werner, N. D., Schade, G. W., and Ying, Q.: Estimation of VOC emission factors from flux measurements using a receptor model and footprint analysis, Atmos Environ, 82, 24-35, 10.1016/j.atmosenv.2013.09.052, 2014.

Kuwata, M., Zorn, S. R., and Martin, S. T.: Using Elemental Ratios to Predict the Density of Organic Material Composed of Carbon, Hydrogen, and Oxygen, Environ. Sci. Technol., 46, 787-794, http://doi.org/10.1021/es202525q, 2012.

~~Lefer, B., Rappengluck, B., Flynn, J., and Haman, C.: Photochemical and meteorological relationships during the Texas-II Radical and Aerosol Measurement Project (TRAMP), Atmos. Environ., 44, 4005-4013, http://doi.org/10.1016/j.atmosenv.2010.03.011, 2010.~~

Leong, Y. J., Sanchez, N. P., Wallace, H. W., Cevik, B. K., Hernandez, C. S., Han, Y., Flynn, J. H., Massoli, P., Floerchinger, C., Fortner, E. C., Herndon, S., Bean, J. K., Hildebrandt Ruiz, L., Jeon, W., Choi, Y., Lefer, B., and Griffin, R. J.: Overview of surface measurements and spatial characterization of submicrometer particulate matter during the DISCOVER-AQ 2013 campaign in Houston, TX, J. Air Waste Manage., 67, 854-872, http://doi.org/10.1080/10962247.2017.1296502, 2017.

Leuchner, M., and Rappengluck, B.: VOC source-receptor relationships in Houston during TexAQS-II, Atmos Environ, 44, 4056-4067, 10.1016/j.atmosenv.2009.02.029, 2010.

Li, J. Y., Cleveland, M., Ziemba, L. D., Griffin, R. J., Barsanti, K. C., Pankow, J. F., and Ying, Q.: Modeling regional secondary organic aerosol using the Master Chemical Mechanism, Atmos. Environ., 102, 52-61, http://doi.org/10.1016/j.atmosenv.2014.11.054, 2015.

Lim, Y. B., Tan, Y., Perri, M. J., Seitzinger, S. P., and Turpin, B. J.: Aqueous chemistry and its role in secondary organic aerosol (SOA) formation, Atmos. Chem. Phys., 10, 10521-10539, http://doi.org/10.5194/acp-10-10521-2010, 2010.

Liu, J. B., Rhland, K. M., Chen, J. H., Xu, Y. Y., Chen, S. Q., Chen, Q. M., Huang, W., Xu, Q. H., Chen, F. H., and Smol, J. P.: Aerosol-weakened summer monsoons decrease lake fertilization on the Chinese Loess Plateau, Nat. Clim. Change, 7, 190-194, http://10.1038/Nclimate3220, 2017.

Mao, J. Q., Ren, X. R., Chen, S. A., Brune, W. H., Chen, Z., Martinez, M., Harder, H., Lefer, B., Rappengluck, B., Flynn, J., and Leuchner, M.: Atmospheric oxidation capacity in the summer of Houston 2006: Comparison with summer measurements in other metropolitan studies, Atmos. Environ., 44, 4107-4115, http://doi.org/10.1016/j.atmosenv.2009.01.013, 2010.

McKeen, S., Grell, G., Peckham, S., Wilczak, J., Djalalova, I., Hsie, E. Y., Frost, G., Peischl, J., Schwarz, J., Spackman, R., Holloway, J., de Gouw, J., Warneke, C., Gong, W., Bouchet, V.,

带格式的: 左, 3 级, 行距: 单倍行距, 到齐到网格

带格式的: 左, 3 级, 行距: 单倍行距, 到齐到网格

1427 Gaudreault, S., Racine, J., McHenry, J., McQueen, J., Lee, P., Tang, Y., Carmichael, G. R.,
1428 and Mathur, R.: An evaluation of real-time air quality forecasts and their urban emissions
1429 over eastern Texas during the summer of 2006 Second Texas Air Quality Study field study,
1430 J. Geophys. Res., 114, D00f11, http://doi.org/10.1029/2008JD011697, 2009.
1431 Middlebrook, A. M., Bahreini, R., Jimenez, J. L., and Canagaratna, M. R.: Evaluation of
1432 Composition-Dependent Collection Efficiencies for the Aerodyne Aerosol Mass
1433 Spectrometer using Field Data, Aerosol Sci. Tech., 46, 258-271,
1434 http://doi.org/10.1080/02786826.2011.620041, 2012.
1435 Olaguer, E. P., Kolb, C. E., Lefer, B., Rappenglueck, B., Zhang, R. Y., and Pinto, J. P.:
1436 Overview of the SHARP campaign: Motivation, design, and major outcomes, J. Geophys.
1437 Res., 119, 2597-2610, http://doi.org/10.1002/2013jd019730, 2014.
1438 Paatero, P., Hopke, P. K., Song, X. H., and Ramadan, Z.: Understanding and controlling
1439 rotations in factor analytic models, Chemometr. Intell. Lab, 60, 253-264,
1440 http://doi.org/10.1016/S0169-7439(01)00200-3, 2002.
1441 Paatero, P., and Tapper, U.: Positive matrix factorization: A non-negative factor model with
1442 optimal utilization of error estimates of data values, Environmetrics, 5, 111-126,
1443 https://doi.org/10.1002/env.3170050203, 1994.
1444 Parrish, D. D., Allen, D. T., Bates, T. S., Estes, M., Fehsenfeld, F. C., Feingold, G., Ferrare,
1445 R., Hardesty, R. M., Meagher, J. F., Nielsen-Gammon, J. W., Pierce, R. B., Ryerson, T. B.,
1446 Seinfeld, J. H., and Williams, E. J.: Overview of the Second Texas Air Quality Study
1447 (TexAQS II) and the Gulf of Mexico Atmospheric Composition and Climate Study
1448 (GoMACCS), J. Geophys. Res., 114, D00f13, http://doi.org/10.1029/2009jd011842, 2009.
1449 Petters, M. D., and Kreidenweis, S. M.: A single parameter representation of hygroscopic
1450 growth and cloud condensation nucleus activity, Atmos. Chem. Phys., 7, 1961-1971, ,
1451 http://doi.org/10.5194/acp-7-1961-2007, 2007.
1452 Petters, M. D., Wex, H., Carrico, C. M., Hallbauer, E., Massling, A., McMeeking, G. R.,
1453 Poulain, L., Wu, Z., Kreidenweis, S. M., and Stratmann, F.: Towards closing the gap
1454 between hygroscopic growth and activation for secondary organic aerosol - Part 2:
1455 Theoretical approaches, Atmos. Chem. Phys., 9, 3999-4009,
1456 http://doi.org/10.5194/acp-9-3999-2009, 2009.
1457 Prenni, A. J., Petters, M. D., Kreidenweis, S. M., DeMott, P. J., and Ziemann, P. J.: Cloud
1458 droplet activation of secondary organic aerosol, J. Geophys. Res., 112, D10223,
1459 http://doi.org/10.1029/2006jd007963, 2007.

Racherla, P. N., and Adams, P. J.: Sensitivity of global tropospheric ozone and fine particulate matter concentrations to climate change, J. Geophys. Res., 111, https://doi.org/10.1029/2005JD006939, 2006.

Rollins, A. W., Smith, J. D., Wilson, K. R., and Cohen, R. C.: Real Time In Situ Detection of Organic Nitrates in Atmospheric Aerosols, Environ. Sci. Technol., 44, 5540-5545, http://doi.org/10.1021/es100926x, 2010.

Rollins, A. W., Browne, E. C., Min, K. E., Pusede, S. E., Wooldridge, P. J., Gentner, D. R., Goldstein, A. H., Liu, S., Day, D. A., Russell, L. M., and Cohen, R. C.: Evidence for NOx Control over Nighttime SOA Formation, Science, 337, 1210-1212, http://doi.org/10.1126/science.1221520, 2012.

Russell, L. M., Takahama, S., Liu, S., Hawkins, L. N., Covert, D. S., Quinn, P. K., and Bates, T. S.: Oxygenated fraction and mass of organic aerosol from direct emission and atmospheric processing measured on the R/V Ronald Brown during TEXAQS/GoMACCS 2006, J. Geophys. Res., 114, D00F05, http://doi.org/10.1029/2008JD011275, 2009.

Schulze, B. C., Wallace, H. W., Bui, A. T., Flynn, J. H., Erickson, M. H., Alvarez, S., Dai, Q., Usenko, S., Sheesley, R. J., and Griffin, R. J.: The impacts of regional shipping emissions on the chemical characteristics of coastal submicron aerosols near Houston, TX, Atmos. Chem. Phys., 18, 14217-14241, http://doi.org/10.5194/acp-18-14217-2018, 2018.

Setyan, A., Zhang, Q., Merkel, M., Knighton, W. B., Sun, Y., Song, C., Shilling, J. E., Onasch, T. B., Herndon, S. C., Worsnop, D. R., Fast, J. D., Zaveri, R. A., Berg, L. K., Wiedensohler, A., Flowers, B. A., Dubey, M. K., and Subramanian, R.: Characterization of submicron particles influenced by mixed biogenic and anthropogenic emissions using high-resolution aerosol mass spectrometry: results from CARES, Atmos. Chem. Phys., 12, 8131-8156, http://doi.org/10.5194/acp-12-8131-2012, 2012.

Sullivan, A. P., Hodas, N., Turpin, B. J., Skog, K., Keutsch, F. N., Gilardoni, S., Paglione, M., Rinaldi, M., Decesari, S., Facchini, M. C., Poulain, L., Herrmann, H., Wiedensohler, A., Nemitz, E., Twigg, M. M., and Collett Jr, J. L.: Evidence for ambient dark aqueous SOA formation in the Po Valley, Italy, Atmos. Chem. Phys., 16, 8095-8108, http://doi.org/10.5194/acp-16-8095-2016, 2016.

Sun, Y. L., Zhang, Q., Schwab, J. J., Demerjian, K. L., Chen, W. N., Bae, M. S., Hung, H. M., Hogrefe, O., Frank, B., Rattigan, O. V., and Lin, Y. C.: Characterization of the sources and processes of organic and inorganic aerosols in New York city with a high-resolution time-of-flight aerosol mass spectrometer, Atmos. Chem. Phys., 11, 1581-1602,

https://doi.org/10.5194/acp-11-1581-2011, 2011.

Sun, Y. L., Du, W., Fu, P. Q., Wang, Q. Q., Li, J., Ge, X. L., Zhang, Q., Zhu, C. M., Ren, L. J., Xu, W. Q., Zhao, J., Han, T. T., Worsnop, D. R., and Wang, Z. F.: Primary and secondary aerosols in Beijing in winter: sources, variations and processes, Atmos. Chem. Phys., 16, 8309-8329, http://doi.org/10.5194/acp-16-8309-2016, 2016.

Surratt, J. D., Gomez-Gonzalez, Y., Chan, A. W. H., Vermeylen, R., Shahgholi, M., Kleindienst, T. E., Edney, E. O., Offenberg, J. H., Lewandowski, M., Jaoui, M., Maenhaut, W., Claeys, M., Flagan, R. C., and Seinfeld, J. H.: Organosulfate formation in biogenic secondary organic aerosol, J. Phys. Chem. A, 112, 8345-8378, http://doi.org/10.1021/jp802310p, 2008.

Tai, A. P. K., Mickley, L. J., and Jacob, D. J.: Correlations between fine particulate matter (PM2.5) and meteorological variables in the United States: Implications for the sensitivity of PM2.5 to climate change, Atmos. Environ., 44, 3976-3984, http://10.1016/j.atmosenv.2010.06.060, 2010.

~~Takegawa, N., Miyakawa, T., Watanabe, M., Kondo, Y., Miyazaki, Y., Han, S., Zhao, Y., van Pinxteren, D., Bruggemann, E., Gnauk, T., Herrmann, H., Xiao, R., Deng, Z., Hu, M., Zhu, T., and Zhang, Y.: Performance of an Aerodyne Aerosol Mass Spectrometer (AMS) during Intensive Campaigns in China in the Summer of 2006, Aerosol Sci. Tech., 43, 189-204, https://doi.org/10.1080/02786820802582251, 2009.~~

Ulbrich, I. M., Canagaratna, M. R., Zhang, Q., Worsnop, D. R., and Jimenez, J. L.: Interpretation of organic components from Positive Matrix Factorization of aerosol mass spectrometric data, Atmos. Chem. Phys., 9, 2891-2918, https://doi.org/10.5194/acp-9-2891-2009, 2009.

~~United States Environmental Protection Agency. National Ambient Air Quality Standards for Particulate Matter, Fed. Reg., 78, 3085–3287, 2013.~~

Wallace, H. W., Sanchez, N. P., Flynn, J. H., Erickson, M. H., Lefer, B. L., and Griffin, R. J.: Source apportionment of particulate matter and trace gases near a major refinery near the Houston Ship Channel, Atmos. Environ., 173, 16-29, https://doi.org/10.1016/j.atmosenv.2017.10.049, 2018.

Watson, J. G.: Visibility: Science and regulation, J. Air Waste Manage., 52, 628-713, http://doi10.1080/10473289.2002.10470813, 2002.

Wood, E. C., Canagaratna, M. R., Herndon, S. C., Onasch, T. B., Kolb, C. E., Worsnop, D. R., Kroll, J. H., Knighton, W. B., Seila, R., Zavala, M., Molina, L. T., DeCarlo, P. F., Jimenez,

J. L., Weinheimer, A. J., Knapp, D. J., Jobson, B. T., Stutz, J., Kuster, W. C., and Williams, E. J.: Investigation of the correlation between odd oxygen and secondary organic aerosol in Mexico City and Houston, Atmos. Chem. Phys., 10, 8947-8968, http://doi.org/10.5194/acp-10-8947-2010, 2010.

Xu, L., Suresh, S., Guo, H., Weber, R. J., and Ng, N. L.: Aerosol characterization over the southeastern United States using high-resolution aerosol mass spectrometry: spatial and seasonal variation of aerosol composition and sources with a focus on organic nitrates, Atmos. Chem. Phys., 15, 7307-7336, http://doi.org/10.5194/acp-15-7307-2015, 2015.

Xu, W. Q., Han, T. T., Du, W., Wang, Q. Q., Chen, C., Zhao, J., Zhang, Y. J., Li, J., Fu, P. Q., Wang, Z. F., Worsnop, D. R., and Sun, Y. L.: Effects of Aqueous-Phase and Photochemical Processing on Secondary Organic Aerosol Formation and Evolution in Beijing, China, Environ. Sci. Technol., 51, 762-770, http://doi.org/10.1021/acs.est.6b04498, 2017.

Ying, Q., Li, J. Y., and Kota, S. H.: Significant Contributions of Isoprene to Summertime Secondary Organic Aerosol in Eastern United States, Environ. Sci. Technol., 49, 7834-7842, http://doi.org/10.1021/acs.est.5b02514, 2015.

Zhang, Q., Jimenez, J. L., Canagaratna, M. R., Ulbrich, I. M., Ng, N. L., Worsnop, D. R., and Sun, Y. L.: Understanding atmospheric organic aerosols via factor analysis of aerosol mass spectrometry: a review, Anal. Bioanal. Chem., 401, 3045-3067, https://doi.org/10.1007/s00216-011-5355-y, 2011.

Zhang, Q. J., Beekmann, M., Freney, E., Sellegri, K., Pichon, J. M., Schwarzenboeck, A., Colomb, A., Bourrianne, T., Michoud, V., and Borbon, A.: Formation of secondary organic aerosol in the Paris pollution plume and its impact on surrounding regions, Atmos. Chem. Phys., 15, 13973-13992, http://doi.org/10.5194/acp-15-13973-2015, 2015.

Zhu, Q., He, L. Y., Huang, X. F., Cao, L. M., Gong, Z. H., Wang, C., Zhuang, X., and Hu, M.: Atmospheric aerosol compositions and sources at two national background sites in northern and southern China, Atmos. Chem. Phys., 16, 10283-10297, http://doi.org/10.5194/acp-16-10283-2016, 2016.

Zorn, S. R., Drewnick, F., Schott, M., Hoffmann, T., and Borrmann, S.: Characterization of the South Atlantic marine boundary layer aerosol using an aerodyne aerosol mass spectrometer, Atmos. Chem. Phys., 8, 4711-4728, http://doi.org/10.5194/acp-8-4711-2008, 2008.

Table 1 Statistics of meteorological parameters, gas-phase pollutants, NR-PM_1 species, and PMF OA factors for the winter and summer campaigns at UHSL.

Variables		Season	Ave. value ± 1 SD	Minimum value	Maximum value
Meteorological parameters	Temp (°C)	Winter	9.3 ± 6.0	0.7	25.9
		Summer	23.6 ± 3.8	12.2	33.1
	RH (%)	Winter	76 ± 18	23	99
		Summer	72 ± 19	21	98
	WS (m s^{-1})	Winter	2.1 ± 1.4	6.8×10^{-3}	9.4
		Summer	2.1 ± 1.2	9.0×10^{-3}	6.7
	Radiometer (W m^{-2})	Winter	0.6 ± 0.9	0.02	3.6
		Summer	1.1 ± 1.3	0.02	4.6
Gas-phase pollutants (ppb)	O_3	Winter	23.0 ± 12.6	0.12	53.0
		Summer	34.9 ± 15.3	0.02	75.9
	CO	Winter	238.7 ± 71.9	98.5	621.1
		Summer	168.3 ± 75.5	103.6	1110.2
	SO_2	Winter	1.0 ± 1.9	5.7×10^{-3}	29.5
		Summer	0.7 ± 1.7	2.8×10^{-3}	30.9
	NO	Winter	4.3 ± 6.4	2.0×10^{-3}	74.9
		Summer	1.3 ± 4.6	0.01	68.1
	NO_2	Winter	12.5 ± 9.7	0.8	101.2
		Summer	4.6 ± 6.4	0.2	44.4
	NO_y	Winter	22.9 ± 19.6	2.8	210.9
		Summer	8.6 ± 11.9	1.3	123.9
NR-PM_1 species (μg m^{-3})	OA	Winter	2.3 ± 1.4	0.42	9.4
		Summer	1.7 ± 1.4	0.27	12.3
	Sulfate	Winter	1.4 ± 0.8	0.05	3.4
		Summer	1.3 ± 0.6	0.02	5.6
	Nitrate	Winter	1.4 ± 1.4	0.02	6.9
		Summer	0.08 ± 0.1	0.01	0.9
	Ammonium	Winter	0.9 ± 0.6	BDL[a]	2.8
		Summer	0.5 ± 0.2	0.02	1.8
	Chloride	Winter	0.06 ± 0.09	BDL	1.1
		Summer	0.02 ± 0.02	BDL	0.5
OA factors (μg m^{-3})	HOA	Winter	0.3 ± 0.4	0[b]	8.6
		Summer	0.2 ± 0.5	0	10.9
	BBOA	Winter	0.6 ± 0.6	0	3.7
		Summer	0.1 ± 0.3	0	5.4
	COA	Winter	0.5 ± 0.5	0	4.8
	LO-OOA	Winter	0.4 ± 0.5	0	2.1
		Summer	0.7 ± 0.9	0	6.7
	MO-OOA	Winter	0.5 ± 0.3	0	1.8
		Summer	0.3 ± 0.2	0	1.6

[a]BDL: below detection limit; [b]Statistically determined factor concentrations with values below $1.0\text{x}10^{-3}$ are listed as 0.

Table 2 Correlation (*r*) of OOA mass spectra with previously published spectra database. (http://cires1.colorado.edu/jimenez-group/HRAMSsd/)

Factor	Winter		Summer		Reference
	MO-OOA	LO-OOA	MO-OOA	LO-OOA	
aq-OOA[a]	**0.96**	0.75	**0.96**	**0.95**	Sun et al., 2016
MO-OOA	0.85	0.87	0.89	0.77	Setyan et al., 2012
MO-OOA	0.98	0.92	0.98	0.60	Hu et al., 2015
LV-OOA	0.97	0.91	0.98	0.62	Crippa et al., 2013
SV-OOA	0.65	0.70	0.70	0.78	Crippa et al., 2013
LO-OOAI, Biogenic-origin	0.83	0.84	0.86	0.76	Hu et al., 2015
LO-OOAII, Anthropogenic-origin	0.78	0.80	0.82	0.74	Hu et al., 2015

[a]aq-OOA is an aqueous-phase-processed SOA reported by Sun et al. (2016); LV=less volatility; SV=semi-volatile.

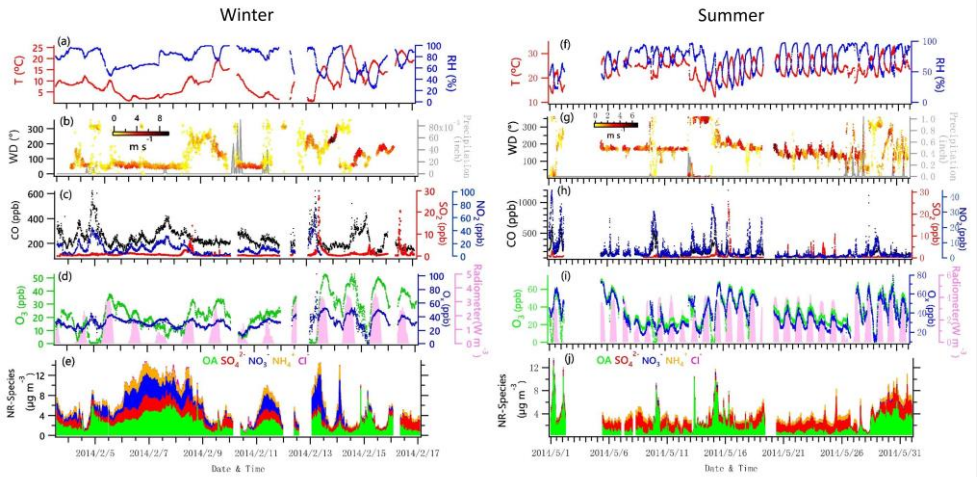

Figure 1. Time series of data collected at UHSL in Houston during the sampling periods in winter and summer 2014. Time series of 5-min average campaign data for **(a, f)** ambient temperature (T) and relative humidity (RH); **(b, g)** precipitation and wind direction (WD), with colors showing different wind speeds (WS); **(c, h)** CO, SO_2 and NO_2; (**d, i**) O_3, O_x (NO_2+O_3) and solar radiometer; **(e, j)** NR-PM_1 species, including OA, NO_3^-, SO_4^{2-}, NH_4^+, and Cl^-.

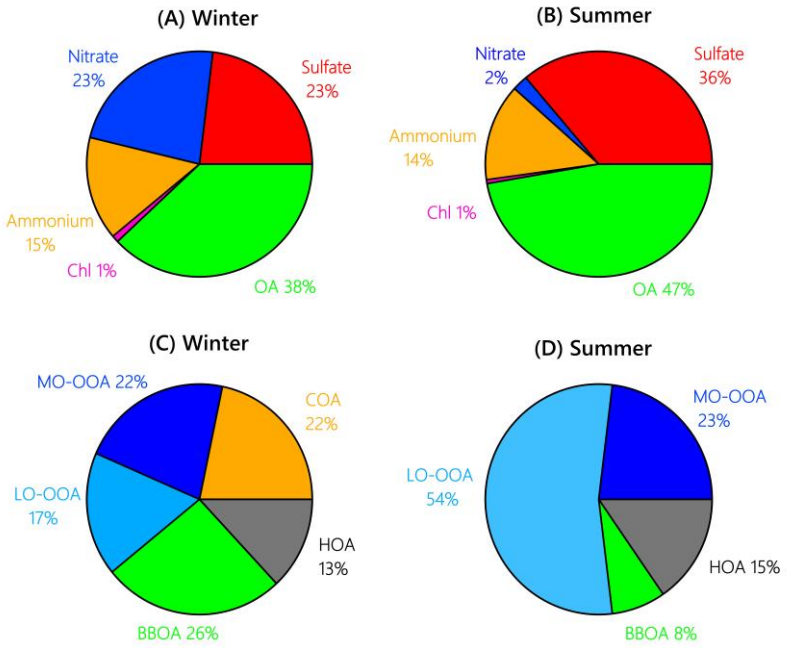

Figure 2. Average composition of NR-PM_1 species and OA factors during the winter (**A, C**) and summer campaign (**B, D**) at UHSL.

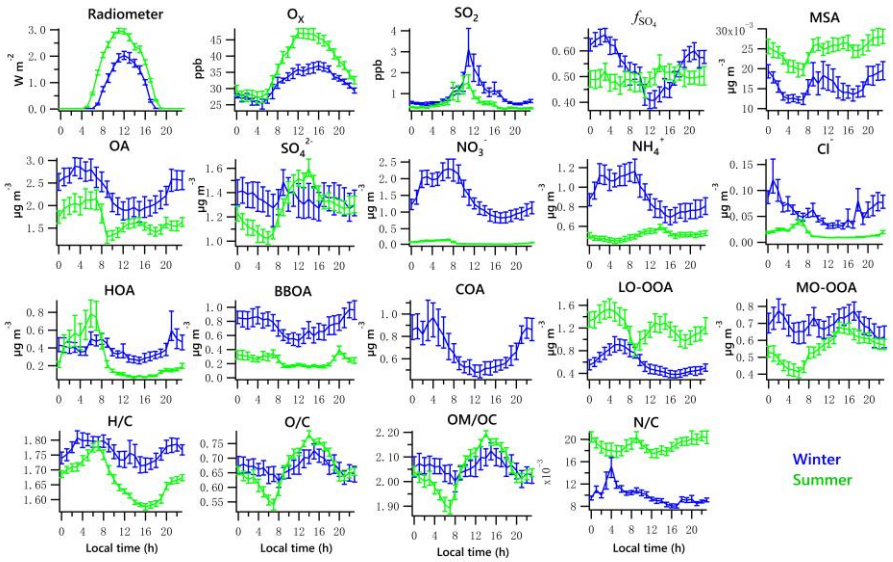

Figure 3. Diurnal profiles of radiometer, O_x, SO_2, f_{SO4}, MSA, each of the five NR-PM_1 species (Org, SO_4^{2-}, NO_3^-, NH_4^+ and Cl^-), PMF-resolved factors (HOA, BBOA, COA, LO-OOA and MO-OOA) and elemental ratios (H/C, O/C, OM/OC and N/C). Lines denote the mean value, and bars represent the 5/95 percent confidence interval in the mean (blue for winter, green for summer).

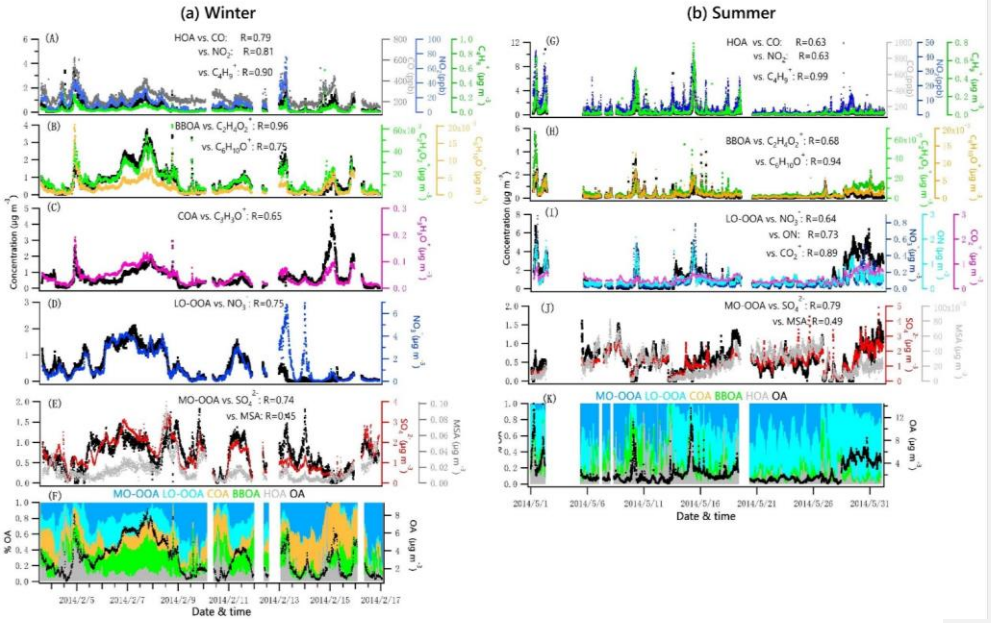

Figure 4. Time series of each OA factor and associated correlated species for the winter and summer campaign at UHSL.

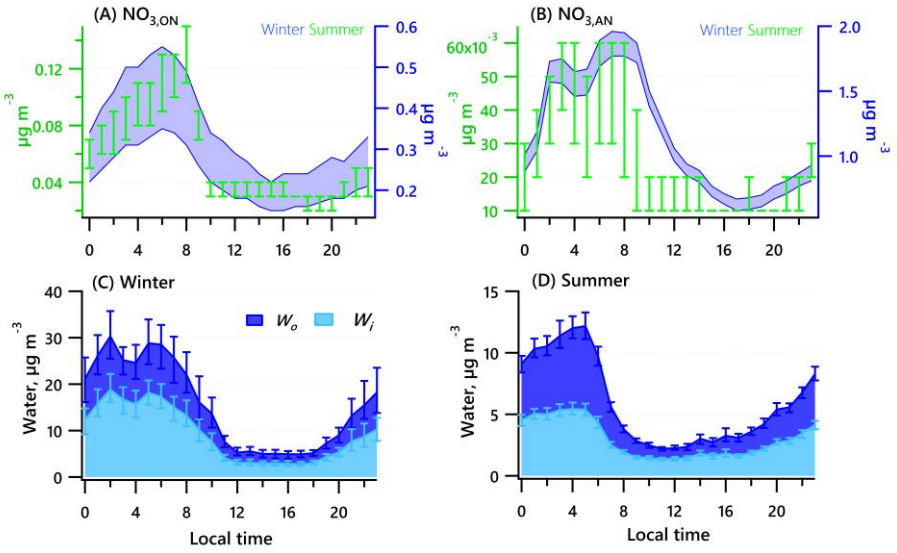

Figure 5. Diurnal profiles of the estimated range of nitrate functionality from organic nitrate (**A**) and inorganic nitrate (**B**) for the winter and summer campaigns. Estimated water associated with inorganic and organic aerosol for the winter (**C**) and summer campaigns (**D**). Solid lines denote the mean value (blue for winter, green for summer), and bars represent the 5/95 percent confidence interval in the mean.

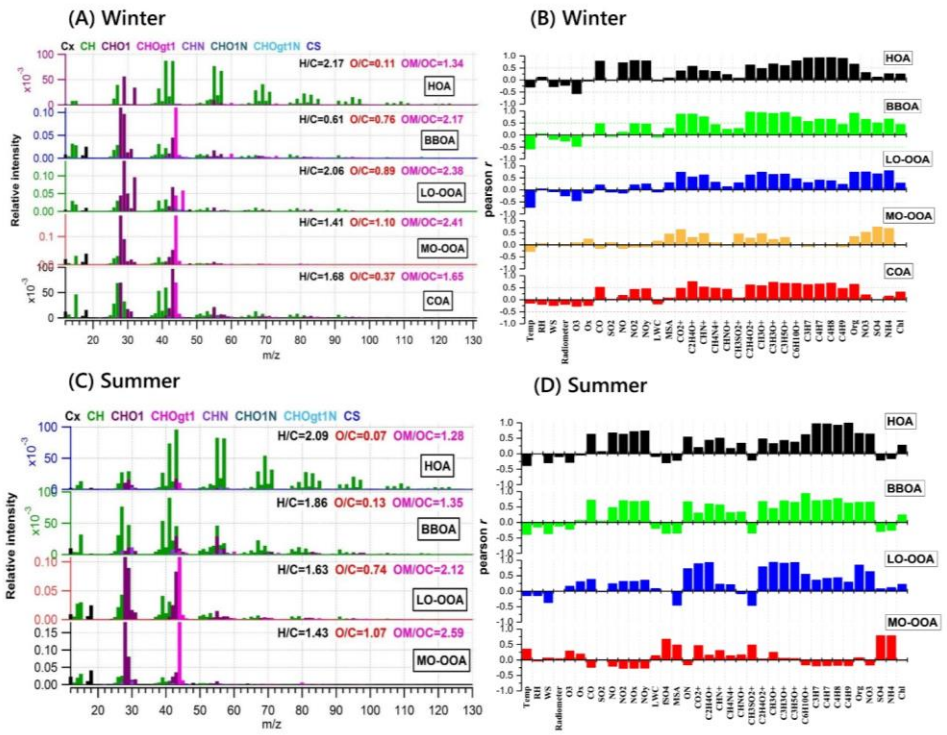

Figure 6. Mass spectra of PMF-resolved OA factors (**A**, **C**) and correlation coefficients between OA factors and other variables (tracer ions, trace gas, meteorological parameters, etc.) (**B**, **D**) for winter and summer campaigns at UHSL.

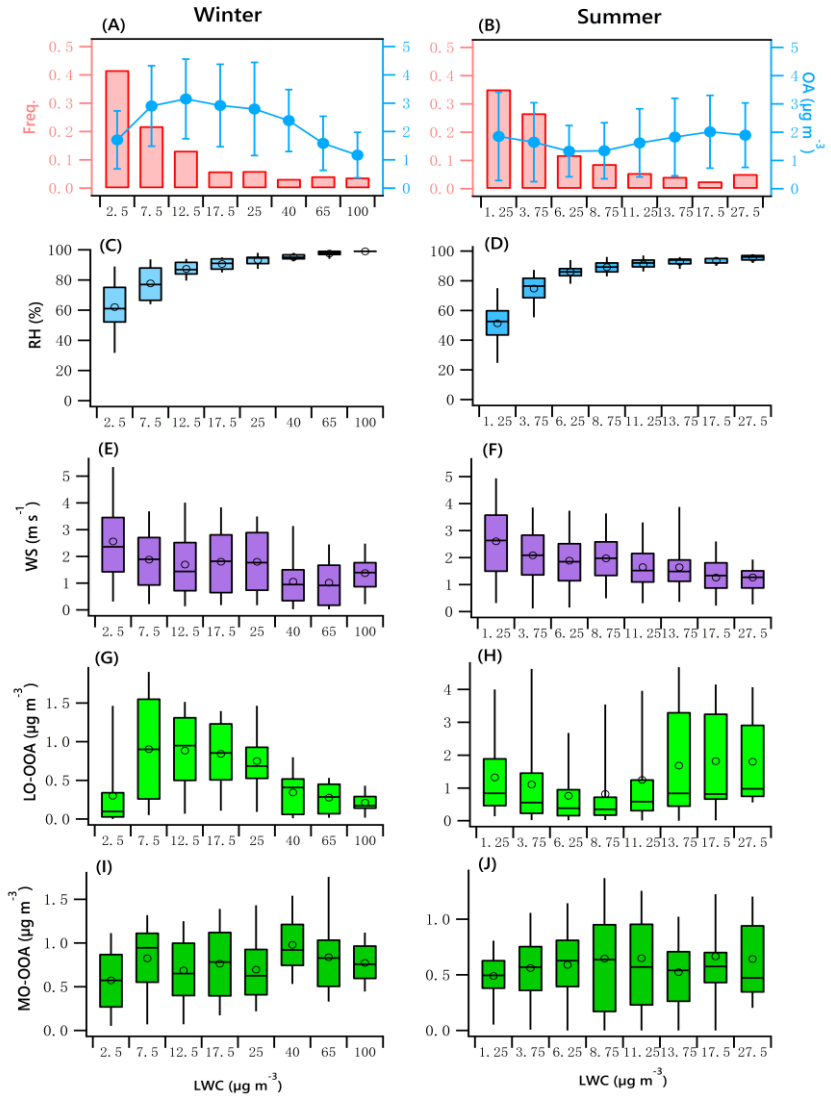

Figure 7. OA mass and frequency histograms of data points in each LWC bin for winter (**A**) and summer (**B**). Variations of RH, WS, LO-OOA and MO-OOA mass as a function of LWC in winter (**C, E, G, I**) and summer (**D, F, H, J**). The data were binned according to the LWC (with different increment values), and mean (circle), median (horizontal line), 25th and 75th percentiles (lower and upper box), and 5th and 95th percentiles (lower and upper whiskers) are displayed for data in each bin.

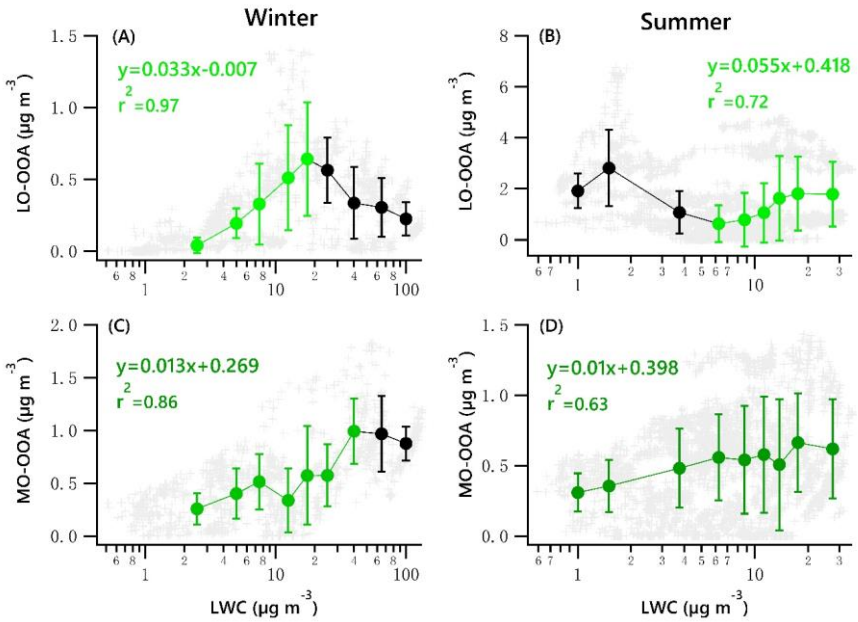

Figure 8. Scatter plots of nighttime OOA vs. LWC for the winter and summer campaign. The linear equations are given for fitting only the green dots. Solid dots denote the average value of data in each bin. Bars indicate standard deviations.

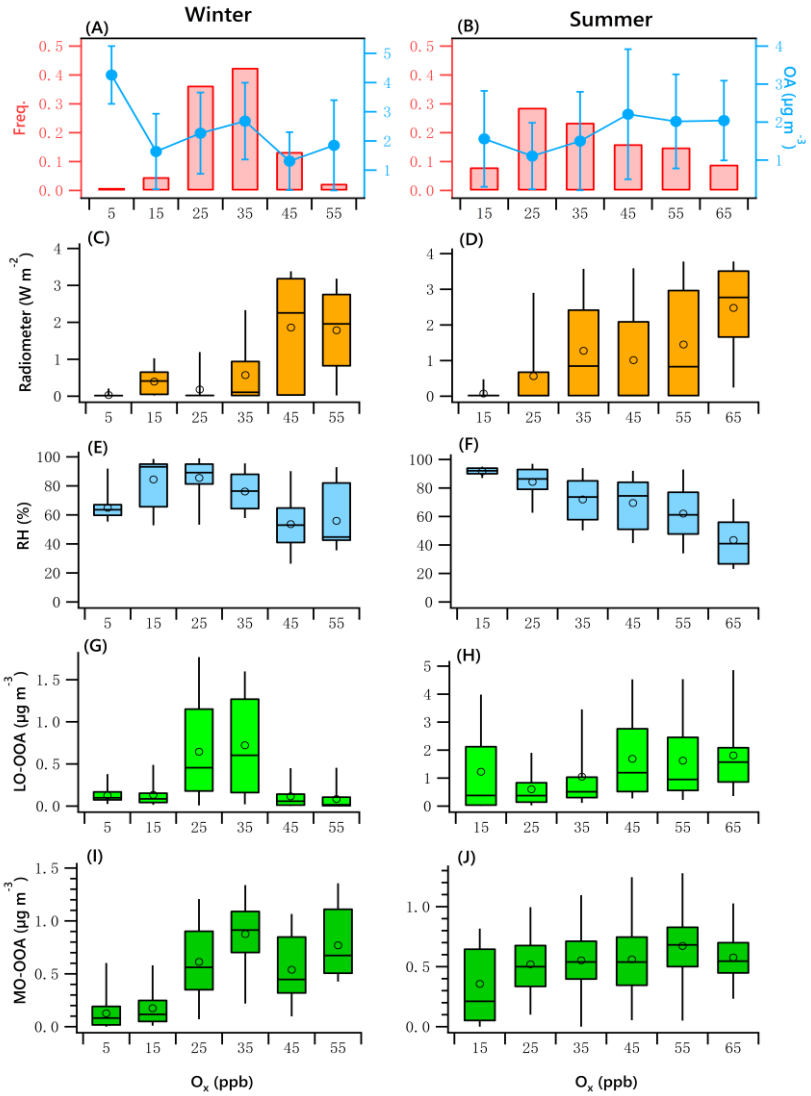

Figure 9. OA mass and frequency histograms of data points in each O_x bin for winter (**A**) and summer (**B**). Variations of solar radiation, RH, LO-OOA and MO-OOA mass as a function of LWC in winter (**C, E, G, I**) and summer (**D, F, H, J**). The data were binned according to the O_x (10 ppb increment), and mean (circle), median (horizontal line), 25th and 75th percentiles (lower and upper box), and 5th and 95th percentiles (lower and upper whiskers) are displayed for data in each bin.

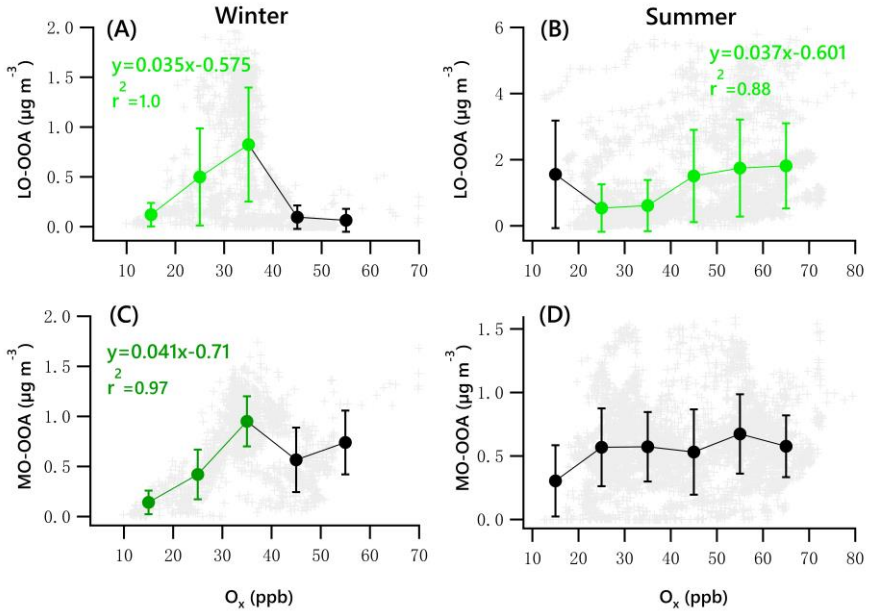

Figure 10. Scatter plots of daytime OOA vs. O_x for the winter and summer campaign. The linear equations are given for fitting the green dots. Bars indicate standard deviations.

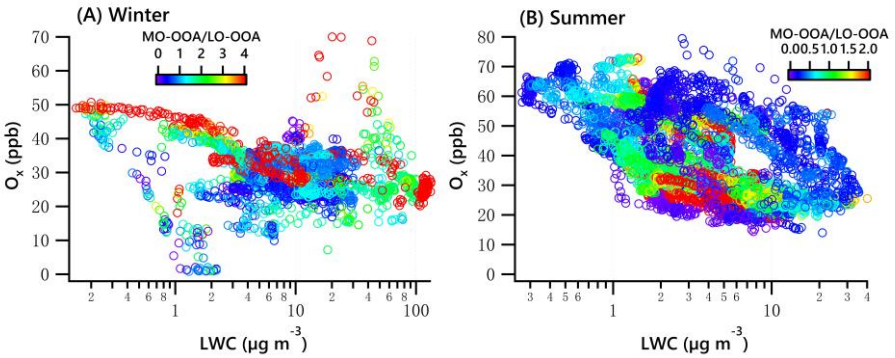

Figure 11. O_x vs LWC dependence of the ratio of MO-OOA/LO-OOA in winter (**A**) and summer (**B**).